João Filipe Pires Ferreira

Licenciado em Ciências de Engenharia Mecânica

Development of an Experimental Setup for Metal Cutting Research

Dissertação para obtenção do Grau de Mestre em

Engenharia Mecânica

Orientador: Jorge Joaquim Pamies Teixeira,
Professor Catedrático, Faculdade de Ciências e Tecnologia da Universidade Nova de Lisboa

Co-orientadora: Carla Maria Moreira Machado,
Professora Auxiliar, Faculdade de Ciências e Tecnologia da Universidade Nova de Lisboa

Júri:

Presidente: Professora Doutora Rosa Maria Mendes Miranda,
Professora Associada com Agregação, Faculdade de Ciências e Tecnologia da Universidade Nova de Lisboa.

Arguente: Professor Doutor Telmo Jorge Gomes dos Santos,
Professor Auxiliar, Faculdade de Ciências e Tecnologia da Universidade Nova de Lisboa.

Vogal: Professor Doutor Jorge Joaquim Pamies Teixeira,
Professor Catedrático, Faculdade de Ciências e Tecnologia da Universidade Nova de Lisboa.

FACULDADE DE CIÊNCIAS E TECNOLOGIA
UNIVERSIDADE NOVA DE LISBOA

Setembro 2015

João Filipe Pires Ferreira

Licenciado em Ciências de Engenharia Mecânica

Development of an Experimental Setup for Metal Cutting Research

Dissertação para obtenção do Grau de Mestre em

Engenharia Mecânica

Orientador: Jorge Joaquim Pamies Teixeira,
Professor Catedrático, Faculdade de Ciências e Tecnologia da Universidade Nova de Lisboa

Co-orientadora: Carla Maria Moreira Machado,
Professora Auxiliar, Faculdade de Ciências e Tecnologia da Universidade Nova de Lisboa

Júri:

Presidente: Professora Doutora Rosa Maria Mendes Miranda,
Professora Associada com Agregação, Faculdade de Ciências e Tecnologia da Universidade Nova de Lisboa.

Arguente: Professor Doutor Telmo Jorge Gomes dos Santos,
Professor Auxiliar, Faculdade de Ciências e Tecnologia da Universidade Nova de Lisboa.

Vogal: Professor Doutor Jorge Joaquim Pamies Teixeira,
Professor Catedrático, Faculdade de Ciências e Tecnologia da Universidade Nova de Lisboa.

Setembro 2015

Development of an Experimental Setup for Metal Cutting Research

Acknowledgments

I want to express my gratitude to everyone that supported and collaborated with this work allowing me fulfill my goals and accomplish another stage in my academic graduation.

First, I would like to manifest my appreciation to Durit for their collaboration and for the resources placed at my disposal. The achievement of this dissertation was only possible due to the customized production of cutting inserts made by this company.

I would like to thank to Professor Pamies Teixeira and Professor Carla Machado for the orientation and support throughout this work. I appreciate all the availability, collaboration and transmitted knowledge. I am grateful for the opportunity to work in this field of research that greatly contributed to the development of my personal skills and knowledge.

Special thanks to Mr. Campos and Mr. Paulo who always helped and followed my workshop work, making possible the construction of the support components presented in this work.

To my friends along the way a special thank for the companionship. Your encouragement allowed each day to be regarded with greater motivation. I would like to make a special reference to Pedro Lopes, who always helped me and encouraged along this work.

I would also like to thank to my family for their efforts to provide me this opportunity and the teachings they gave me that led me this far. All the achievements I make are theirs.

Finally, I would like to dedicate this work to Diana who always transmitted confidence and powers, helping me reach the beginning of a new journey.

Abstract

Analytical, numerical and experimental models have been developed over time to try to characterize and understand the metal cutting process by chip removal. A true knowledge of the cutting process by chip removal is required by the increasing production, by the quality requirements of the product and by the reduced production time, in the industries in which it is employed.

In this thesis an experimental setup is developed to evaluate the forces and the temperature distribution in the tool according to the orthogonal cutting model conditions, in order to evaluate its performance and its possible adoption in future works. The experimental setup is developed in a CNC lathe and uses an orthogonal cutting configuration, in which thin discs fixed onto a mandrel are cut by the cutting insert.

In this experimental setup, the forces are measured by a piezoelectric dynamometer while temperatures are measured by thermocouples placed juxtaposed to the side face of the cutting insert. Three different solutions are implemented and evaluated for the thermocouples attachment in the cutting insert: thermocouples embedded in thermal paste, thermocouples embedded in copper plate and thermocouples brazed in the cutting insert.

From the tests performed in the experimental setup it is concluded that the adopted forces measurement technique shows a good performance. Regarding to the adopted temperatures measurement techniques, only the thermocouples brazed in the cutting insert solution shows a good performance for temperature measurement. The remaining solutions show contact problems between the thermocouple and the side face of the cutting insert, especially when the vibration phenomenon intensifies during the cut. It is concluded that the experimental setup does not present a sufficiently robust and reliable performance, and that it can only be used in future work after making improvements in the assembly of the thermocouples.

Keywords: Experimental Setup; Orthogonal Cutting; Forces Measurement; Temperature Measurement; Thermocouple.

Resumo

Vários modelos analíticos, numéricos e experimentais têm sido desenvolvidos ao longo dos tempos para tentar caracterizar e compreender o processo de corte de metal por arranque de apara. Um verdadeiro conhecimento do processo de corte por arranque de apara é exigido pelo crescente aumento de produção, pelas exigências de qualidade do produto e pelo reduzido tempo de produção, nas indústrias onde está presente.

Na presente dissertação desenvolve-se uma montagem experimental para avaliar as forças e a distribuição de temperatura na ferramenta segundo as condições do modelo de corte ortogonal, com o propósito de avaliar a sua performance e possível adopção em trabalhos futuros. A montagem experimental é desenvolvida num torno CNC e utiliza uma configuração de corte ortogonal em que discos finos, fixos num mandril, são cortados pelo inserto de corte.

Nesta montagem experimental, as forças são medidas por um dinamómetro piezoeléctrico enquanto as temperaturas são medidas por termopares colocados justapostos à face lateral do inserto de corte. São implementadas e avaliadas três soluções diferentes de fixação dos termopares no inserto de corte: termopares embebidos em pasta térmica, termopares embebidos em chapa de cobre e termopares brasados no inserto de corte.

Dos ensaios realizados na montagem experimental conclui-se que a técnica de medição de forças adoptada mostra um bom desempenho. Relativamente às técnicas de medição de temperaturas adoptadas, apenas a solução dos termopares brasados no inserto de corte apresenta uma boa performance de medição de temperatura. As restantes soluções apresentam problemas de contacto entre os termopares e a superfície lateral do inserto de corte, sobretudo quando o fenómeno de vibração se intensifica no decorrer do corte. Conclui-se que a montagem experimental não apresenta uma performance suficientemente robusta e fiável, e que a sua utilização em trabalhos futuros só é possível após a introdução de melhorias na fixação dos termopares.

Palavras-chave: Montagem Experimental; Corte Ortogonal; Medição de Forças; Medição de Temperaturas; Termopar.

Contents

List of Figures

List of Tables

List of Abbreviations and Symbols

α	Rake Angle
β	Clearance Angle
γ_{EF}	Shear Strain at EF
Δk	Change in Shear Flow Stress in the Parallel-Sided Shear Zone
Δs_2	Thickness of the Parallel-Sided Shear Zone
θ	Useful Angle
λ	Friction Angle
λ_C	Thermal Conductivity
μ	Friction Coefficient
Φ	Shear Angle
φ	Oblique Angle
A_C	Cutting Area
a_C	Thermal Diffusivity
A_S	Area of the Cutting Plane
b	Cutting Width
CNC	Computer Numerical Control
dl_i	Differential Segments
F	Friction Force
F_C	Cutting Force
F_N	Force Perpendicular to F_S
F_S	Shearing Force
F_T	Thrust Force
k_0	Shear Flow Stress at Zero Plastic Strain

K_0 Bessel Function of the Second Kind and Zero Order

k_{AB} Shear Flow Stress on AB

l Length of AB

m Slope of Linear Plastic Stress-Strain Relation

N Normal Force

q Heat Liberation Intensity of the Heat Source

R Force that the Workpiece Exerts on the Base of the Chip

R’ Force that the Tool Exerts on the Chip Back Surface

t_1 Undeformed Chip Thickness

V Velocity of Moving Plane Heat Source

V_C Cutting Velocity

V_{Chip} Chip Velocity

V_N Normal Component of V_C in the Perpendicular Direction to the Shear Plane

V_S Shear Velocity

1 Introduction

This chapter provides an introduction to this dissertation. Here are presented the work context, the motivation, the established goals, as well as the structure of the dissertation.

1.1 Context

Nowadays, the increase of product quality requirements at levels of high productivity implies that the manufacturing processes must be executed more efficiently. Regarding the machining processes, they represent a dominant fraction of all manufacturing operations [1]. The conventional machining processes, as turning, drilling or milling, stand out between the technological processes of parts manufacturing due to their capability to process complex geometries with tight tolerances and to produce a high quality level of surface finish. In fact, the metal machining by chip formation processes are commonly used in the production of the final shape of mechanical components [2]. Consequently, arises the need of better understand the cutting process in order to optimize the machining processes.

One of the major problems in the metalworking industry is the heat generated during the cutting process [3]. In fact, the maximum temperatures generated on the tool rake face or on the tool clearance face will determine the life of the cutting tool [4]. The temperature at the tool-workpiece interface rises with cutting speed [5], and as a result of this temperature rise the tool wear increases. The evolution of machining technology and the development of new tool materials depend on understanding the cutting temperatures on the tool material, and its influence on the tool life and on the tool performance [4]. On the other hand, the high temperatures in metal cutting degrade the surface integrity, and reduce the size accuracy and the machining efficiency [3]. Moreover, the maximum temperature, the temperature gradient and the rate of cooling of the workpiece are process variables that influence the subsurface deformation, the metallurgical structural alterations in the machined surface, and the residual stresses in the finished piece [4]. For these reasons, the amount of heat generated, during the cutting process, and the consequent temperature rise (maximum and average) are process variables that are necessary to understand in order to optimize the cutting process.

For these reasons, different approaches have been made over time, such as the development of analytical models, numerical models and experimental models, with the aim of describe this thermal phenomenon of the cutting process. Although all the different types of models are

relevant, the experimental models stand out because they perform the connection between the theoretical models and the thermal phenomenon itself. Actually, the experimental setups developed in experimental models are the validation instrument of analytical and numerical models, and, as a result, the experimental setups have an important role in the improvement of theoretical models. On the other hand, the nonexistence of commercial equipment that assesses temperature during the cutting process is a gap that can be overcome by the research and development of robust and reliable experimental setups. In conclusion, the measurement of temperature in material removal processes is a key to understand the performance of material removal processes and the quality of the workpiece [5].

1.2 Objective

The main purpose of this dissertation is the development of an experimental setup to evaluate the forces and the tool temperature distribution in the orthogonal cutting process of metal, which arises from the need to establish a connection between an existing predictive analytical and numerical model for orthogonal cutting [6] and the direct evaluation of temperature distribution in the tool, by using the equipment available on the mechanical technology laboratory. Thus, the objectives are the development and implementation of the adopted forces measurement technique and of the adopted temperature measurement techniques, the evaluation of the performance of the experimental setup and the conclusion about its possible adoption in future experimental investigations in metal cutting.

1.3 Contents

The structure of this dissertation is divided in four parts: Introduction, State of the Art, Experimental Work and Conclusions. This first chapter provides a global view of the dissertation, focusing on the theme contextualization and justification, as well as on the presentation of the proposed objectives. In addition, this first chapter presents the structure of the document.

In Chapter 2 is presented the outcome of the bibliographic research accomplished. It contains the theoretical principles of the theme of the dissertation and a literature review that comprises the state of the art relevant to this work. This chapter is divided in four fundamental points: the orthogonal cutting model, the mechanics of machining, the thermodynamics of machining and the experimental methods for forces and temperature measurements in metal cutting.

The Experimental Work is developed in the third chapter and in the fourth chapter. In Chapter 3 is presented the temperature measurement method and the force measurement method applied, together with the required procedures for their application. This chapter also covers the definition of the experimental procedures, including the selection of test materials and the methodology applied during tests. Next, in Chapter 4 are presented and discussed the results of the experimental setup performance.

Finally, Chapter 5 presents the main conclusions of the dissertation as well as proposals for future work.

2 Background

2.1 Orthogonal Cutting Model

In analytical and experimental research investigations of chip formation it is usual to consider the relatively simple case of orthogonal cutting (Figure 2.1a) [7]. The orthogonal cutting model is a two-dimensional problem, allowing the elimination of several independent variables. The term "orthogonal cutting" refers to the case where the tool cutting edge is arranged to be perpendicular to the direction of tool-workpiece relative motion, wherein the cutting tool generates a plane face parallel to an original plane surface of the cut material [8]. Although these cutting conditions do not represent a large number of applications, the orthogonal cutting model presents a solid foundation for explaining the set of practical observations, providing the basis for machining mechanics development.

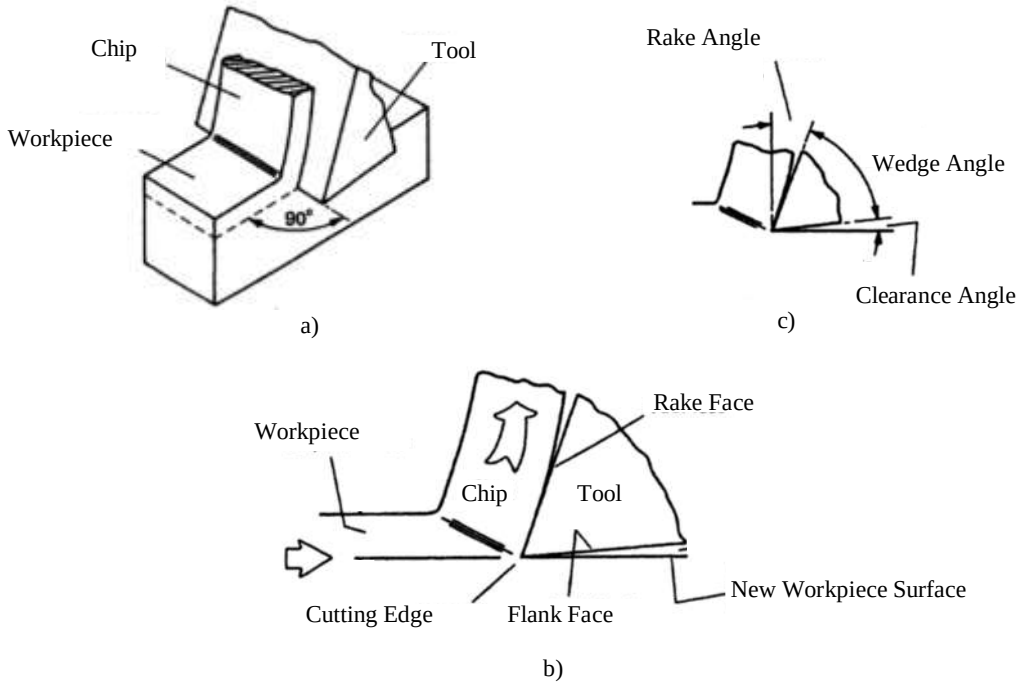

Figure 2.1 - Orthogonal Cutting: a) Model b) Surfaces and parts c) Angles;
Adapted from [9]

In the orthogonal cutting model the surface through which the chip flows is known as the tool rake face, whereas the surface which overlaps the machined material is known as the tool flank face (Figure 2.1b). The cutting edge is defined as the theoretical line of intersection of the rake face with the flank face, and it is considered to be perfectly sharp. Regarding to the angles

formed between surfaces (Figure 2.1c), the rake angle (α), which is the angle between the rake face and a line perpendicular to the new workpiece surface, and the clearance angle (β), which is the angle between the flank face and the new workpiece surface, are the most relevant. However, it can also be defined a third angle designated as the wedge angle, which is the angle between the rake face and the flank face.

In literature it can be found several experimental setups with different configurations for the orthogonal cutting. Hastings (1967) [10] developed a quick and stop device, designed for using in a shaping machine, which enables to suddenly stop the cutting action and allows subsequent microscopic examination of the chip formation process. Using this device, the author studied the plastic flow fields in metal cutting. In a common quick and stop device, the workpiece is gripped in a clamping tool, which is free to slide in the guide block (Figure 2.2) [9]. During the cutting operation, the clamping tool is pushed against the holding ring, which is held in position by the action of shear pins that are mechanical fuses designed to support the force required to remove the chip and cross through the guide block and the holding ring. When the cutting is nearly completed, a tongue collides against the clamping tool shearing the pins, and as a result the clamping tool and the holding ring move freely. Lastly, the action of the tongue stops the cutting action, because it accelerates the speed of the workpiece in relation to the speed of the cutting tool.

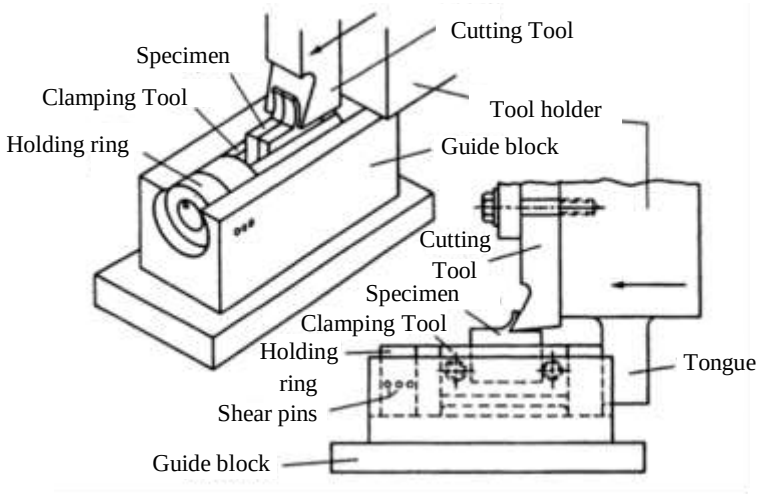

Figure 2.2 - Quick and Stop Device
Adapted from [9]

A different configuration presented in literature consists in orthogonal cutting machining of thin discs [7], [11], [12], [13] in which the workpiece is clamped in a mandrel (which in turn is held by the lathe chuck) and the cutting edge of the tool is normal to the cutting and feed

directions (Figure 2.3). Stevenson and Oxley (1969-1970) [7] developed a quick and stop device using this configuration, by clamping three discs together in the mandrel in order to obtain strain plane conditions on the center disc. These authors used this quick and stop device together with a printed grid to measure the deformation in the chip formation zone, and with the obtained results they studied the influence of cutting speed and undeformed chip thickness on the size of the chip formation and the strain-rates in this zone. In contrast, the orthogonal cutting of thin discs was also applied to evaluate the temperature distribution in the cutting tool during the machining process [13].

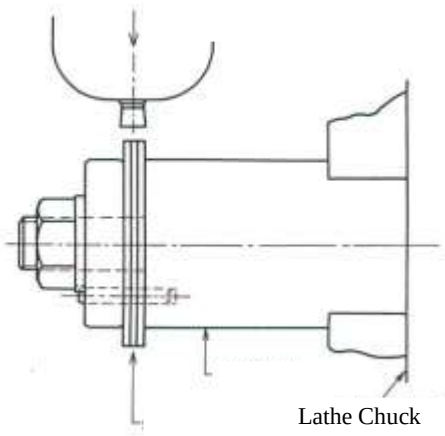

Figure 2.3 - Orthogonal Machining of Thin Discs
Adapted from [7]

Another experimental setup was developed by Boothroyd (1963), who applied an infrared photo-graphic technique to measure the temperature distribution in the workpiece, chip and tool in orthogonal cutting [14]. This experimental setup was performed in a lathe, where a long tube was cut with a cutting direction parallel to the rotation axis of the tube (Figure 2.4).

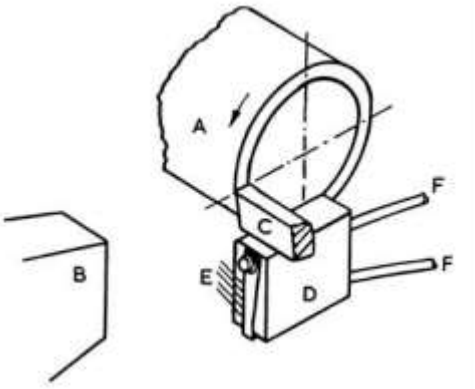

Figure 2.4 - Orthogonal Machining of a Long Tube
Adapted from [4]

Boothroyd's method involved the photography of the workpiece, the tool and the chip using an infrared sensitive photographic plate and the measurement of the optical density of the plate with a microdensitometer, and additionally, a heat tapered strip was mounted next to the tool, where thermocouples were distributed, being photographed simultaneous with the process [4].

2.2 Mechanics of Machining

In mechanics of machining research the subject under study is the basic chip formation process by which the material is removed from the workpiece [7]. The complex flow of the chip material, which occurs in the shear deformation zone, is a basic and important characteristic of machining processes. The machining processes characteristics can be understood provided that the rules of the chip material flow are known, and furthermore the acceptable models for machining must satisfy stress equilibrium and velocity requirements of the flow of the chip material [15].

The investigation in metal cutting started approximately seventy years after the introduction of the first machine tool, but only a few years later was suggested by Mallock (1881), an acceptable model (Figure 2.5) describing the cutting process as the shearing of the work material and highlighting the friction effect that occurs on the cutting-tool face, whose concepts remain similar to those of modern models, like the well-known model of Ernst and Merchant [9]. Their shear plane model is a reference to most of the works on metal cutting mechanics and many analytical models of orthogonal cutting, where the relations derived from their work are used [16].

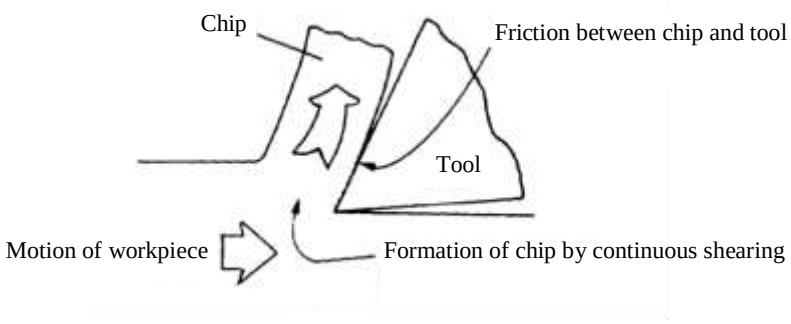

Figure 2.5 - Mallock's Model
Adapted from [9]

It is generally considered the existence of two distinct zones where the plastic deformation takes place, namely the primary deformation zone and the secondary deformation zone (Figure 2.6). The primary deformation zone is the area contained between OAB, where the workpiece

material enters, by crossing the OA boundary, and undergoes deformation at high strain rates. As a result, the material becomes work hardened, and lastly exits the zone at the OB boundary. On the other hand, the secondary deformation zone is included in OCD, in which along OD, where the rake face and the chip are in contact, the material is deformed due to interfacial friction. The secondary deformation zone is composed by two distinct regions the sticking zone, which is close to the cutting tool and it is where the material adheres to the tool, and the sliding zone, which is above the previous one.

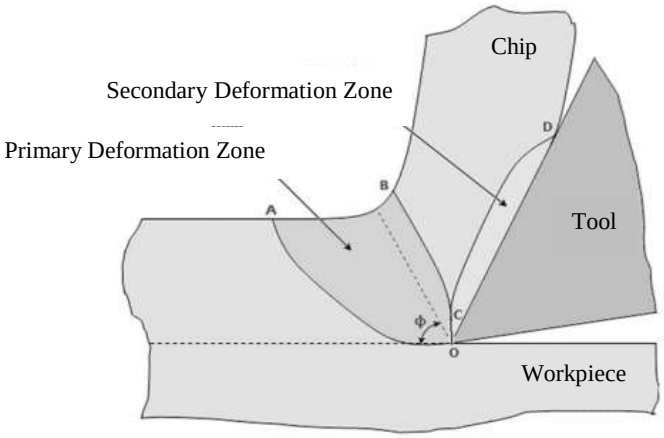

Figure 2.6 - Deformation Zones
Adapted from [16]

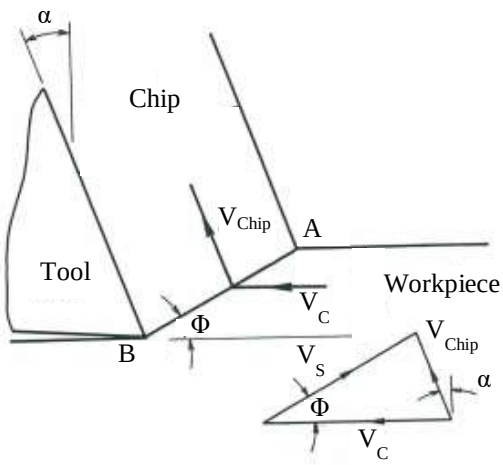

Figure 2.7 - Velocities Diagram
Adapted from [7]

According to Merchant's research (1945) [8], a continuous chip is formed by plastic deformation in a narrow region that runs from the cutting edge to the workpiece free surface (from A to B) (Figure 2.7). This region is termed as the shear plane and the angle formed

between the shear plane and the new workpiece surface is the shear angle (Φ). Assuming the tool is stationary, it is in the shear plane where the cutting velocity (V_C) instantaneously changes to the chip velocity (V_{Chip}), due to a discontinuity in the tangential component of the cutting velocity equal to the velocity of shear (V_S). The velocity V_N is the normal component of V_C in the perpendicular direction to the shear plane. From the velocities diagram the following expressions can be established:

$$V_{Chip} = \frac{\sin \Phi}{\cos(\Phi - \alpha)} \cdot V_C \tag{2.1}$$

(2.2)

$$V_S = \frac{\cos \alpha}{\cos(\Phi - \alpha)} \cdot V_C \tag{2.3}$$

(2.4)

$$V_N = \sin \Phi \cdot V_C \tag{2.5}$$

Concerning to the forces involved in the cutting process, this research considered the chip as a separate body in equilibrium under the action of two equal and opposite resultant forces, the force which the tool exerts on the chip back surface (R') and the force which the workpiece exerts on the base of the chip (R) (Figure 2.8). The force R may be decomposed along the shear plane into a component F_S, the shearing force, which is responsible for the work expended in the shearing, and into a component F_N, which is perpendicular to F_S and exerts a compressive stress in the shear plane. Beyond this direction, the force R may be also decomposed along the direction of motion of the tool relative to the workpiece (cutting direction), into a component F_C, the cutting force, which is responsible for cutting the material, and into a component F_T, the thrust force, which is perpendicular to F_C and according to feed direction. Similarly, the force R' may be decomposed along the rake face into a component F, the friction force, which is related to the friction work, and into a component N, the normal force, perpendicular to F. Regarding to the angle formed between the normal force and the force exerted by the tool on the chip, it is denominated as friction angle (λ) and describes the frictional condition in the tool-chip interface. From the forces diagram the following expressions can be established:

$$F_C = R \,.\cos(\lambda - \alpha) \tag{2.6}$$

$$F_T = R \,.\sin(\lambda - \alpha) \tag{2.7}$$

$$F = R\,.\sin(\lambda) = F_C.\frac{\sin(\lambda)}{\cos(\lambda-\alpha)} \tag{2.8}$$

$$N = R\,.\cos(\lambda) = F_C.\frac{\cos(\lambda)}{\cos(\lambda-\alpha)} \tag{2.9}$$

$$F_S = R.\cos(\Phi+\lambda-\alpha) = F_C.\frac{\cos(\Phi+\lambda-\alpha)}{\cos(\lambda-\alpha)} \tag{2.10}$$

$$F_N = R.\sin(\Phi+\lambda-\alpha) = F_C.\frac{\sin(\Phi+\lambda-\alpha)}{\cos(\lambda-\alpha)} \tag{2.11}$$

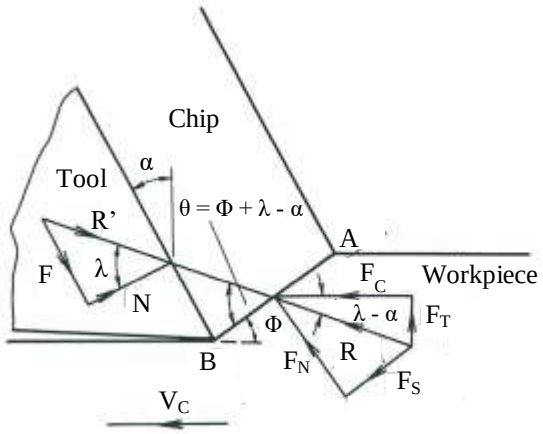

Figure 2.8 - Forces Diagram
Adapted from [7]

Despite the rake angle and clearance angle, which are geometrical parameters of the tool, are known, the shear angle and friction angle, which depend on the cutting conditions, have been a source of scientific investigation and proposed theories. Early attempts were made by Piispanen (1937), however the first complete shear plane model was presented by Ernst and Merchant (1941). Based on a velocities diagram and a forces diagram equal to the above cited from Merchant's research [8], and also assuming that the workpiece material was perfectly plastic and homogeneous, Ernst and Merchant established the assumption that the shear angle would take a value that maximizes the shear stress in the shear plane. Considering an uniform stress distribution along the shear plane, the normal stress and the shear stress are given by:

$$\tau_S = \frac{F_S}{A_S} = \frac{R}{b.t_1}\cdot\cos(\Phi+\lambda-\alpha)\cdot\sin(\Phi) \tag{2.12}$$

$$\sigma_S = \frac{F_N}{A_S} = \frac{R}{b.t_1} \cdot \sin(\Phi + \lambda - \alpha) \cdot \sin(\Phi) \tag{2.13}$$

Equally important, the area of the cutting plane (A_S) is determined by:

$$A_S = \frac{A_C}{\sin(\Phi)} = \frac{b.t_1}{\sin(\Phi)} \tag{2.14}$$

Where the cutting area (A_C) is given by the product between the cutting width (b) and the undeformed chip thickness (t_1). By differentiating the shear stress with respect to the shear angle, the value of the shear angle that maximizes the shear stress can be calculated, and this is given by:

$$\Phi = \frac{\pi}{4} + \frac{\alpha - \lambda}{2} \tag{2.15}$$

Where the friction angle, knowing beforehand the friction coefficient (μ), is given by:

$$\mu = \tan(\lambda) \tag{2.16}$$

However this model is only valid for an idealized rigid-perfectly plastic work material (non-work-hardening), for which the elastic strain and volume variations of the elements in the material are not regarded. Indeed, the equation poorly agreed with experimental investigation of metal machining.

Most of the shear plane models consider that the shear stress is uniformly distributed along the shear plane and that the friction coefficient is constant, whereas the material strain hardening is not considered, wherein this last assumption is in contradiction with experimental investigation [16]. By assuming that deformation takes place in a narrow zone centered on the shear plane, more general assumptions about the material can be stated. Considering that the conservation of mass occurs, it requires that the normal component of velocity is continuous across the shear plane, implying the chip velocity to be equal to the normal component of the cutting velocity in the perpendicular direction to the shear plane. The shear plane is the plane of tangential discontinuity, and consequently the direction of maximum shear strain rate. Therefore, considering the isotropic plasticity theory the shear plane may be regarded as the direction of

maximum shear stress. However, if the material hardens during the deformation the discontinuity in tangential velocity is no longer acceptable. Thereby, in this case the shear plane becomes a shear zone.

Oxley introduced an analytical model known as the parallel-sided shear zone [7] (Figure 2.9). The overall geometry of the shear zone model is similar to the shear plane model from Ernst and Merchant, with AB and Φ being equivalent to the shear plane and the shear angle, respectively. On this model, the shear plane is assumed to be open at two boundaries, an upper boundary between the shear plane and the chip (EF) and a lower boundary between the shear plane and the workpiece (CD), which are both parallel and equidistant from the shear plane. This model assumes that the cutting velocity changes to the chip velocity, in the shear zone, along smooth and geometrical identical streamlines, without velocity discontinuities. Although the velocities diagram (Figure 2.7), the forces diagram (Figure 2.8) and equations remain equal, in general, the resultant force (R) will not pass through the midpoint of the shear plane.

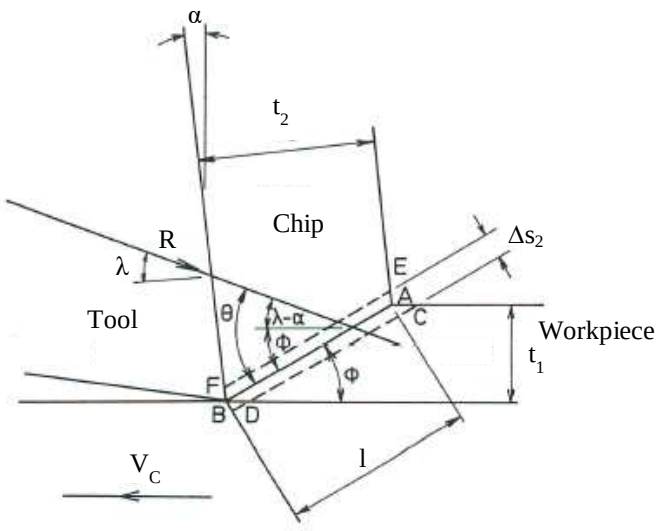

Figure 2.9 - Parallel-sided Shear Zone Model
Adapted from [7]

The methodology applied in the parallel-sided shear zone model consists in the determination of the stresses along AB, in terms of the shear angle and the work material properties, in order to determine the magnitude and direction of the resultant force R transmitted by AB. Considering that the tool is perfectly sharp, the shear angle is determined so that the resultant force is consistent with the frictional conditions at the tool-chip interface. From the assumptions made, it was stated that the shear strain is constant along AB, as well as the shear strain along CD and

the shear strain along EF [7]. Based in the slip line analysis of experimental flow fields, Oxley stablished the following equation:

$$\tan(\theta) = 1 + 2\left(\frac{\pi}{4} - \phi\right) - \frac{\Delta k}{2k_{AB}}\frac{l}{\Delta s_2} \tag{2.17}$$

Where Δs_2 is the thickness of the shear zone and θ the useful angle that may be expressed by:

$$\theta = \phi + \lambda - \alpha \tag{2.18}$$

To relate the change in shear flow stress in the parallel sided shear zone (Δk) and the shear stress on AB (k_{AB}) to the shear flow stress-shear strain curve of the work material, the author assumed:

$$\Delta k = m\,.\,\gamma_{EF} \tag{2.19}$$

Where m is the slope of the stress-strain curve and γ_{EF} is the shear strain along EF. The shear strain along EF is given by:

$$\gamma_{EF} = \frac{\cos(\alpha)}{\sin(\phi)\,.\cos(\phi - \alpha)} \tag{2.20}$$

Finally, assuming that half of the strain takes place at AB it was determined the following equation:

$$k_{AB} = k_0 + \frac{1}{2}\,.m\,.\,\gamma_{EF} \tag{2.21}$$

Where k_0 is the shear flow stress at zero plastic strain, which is equal to k_{CD}.

Concluding, for given values of α, λ and t_1 it is possible to determine Φ from equation 2.17 to equation 2.21, if correct values of Δs_2, k_0 and m are known. Then, Φ can be used to calculate the cutting forces equations.

2.3 Thermodynamics of Machining

When the work material is elastically deformed, the energy is stored in the material as strain energy and no heat is generated. By contrast, when the work material is deformed plastically most of the energy is converted into heat, which propagates by conduction and convection mechanisms, although the predominant mechanism is conduction. For this reason, the temperature rises in the chip, in the tool and, more slightly, in the workpiece. Usually, is considered that conversion of energy into heat occurs in the two principal regions of plastic deformation (Figure 2.6), the primary deformation zone and the secondary deformation zone.
The heat generated in metal cutting was one of the first and the foremost subject investigated in machining [17]. The study of temperature distribution attracted many researchers due to its complexity, and different approaches were made in order to comprehend and describe the thermodynamics of machining. Among the analytical models of machining temperatures, the main differences between these models are the assumptions made, such as the origin and type of the heat source, the direction of motion of the heat source, the boundary conditions and also the estimation of heat partition ratio. The majority of these models assume that the material on both sides of the shear plane is constituted by two separate bodies in sliding contact, however Hahn and Chao and Trigger assumed it correctly as a single body [17].

Chao and Trigger (1951) [18] developed a steady state two dimensional analytical model, in which they calculated the average temperature rise of the chip as it leaves the shear plane, due to the primary deformation zone, and the average tool chip interface temperature in orthogonal cutting, based on the existence of two plane heat sources in which the energy is uniformly distributed, one in the primary deformation zone and the other in the secondary deformation zone. They assumed that the latent heat stored in the chip was approximately 12,5% and that 90% of the heat flow into the chip, while the remaining 10% flows into the work material. Besides, they assumed that there was no redistribution of the thermal shear energy going to the chip during the very short time the chip was in contact with the tool, and the thermal energy distribution at the shear plane was computed by using Block's partition principle. The friction heat source was considered as a moving band heat source in relation to the chip and as a stationary plane source in relation to the tool, with the work surface and the machined surface considered as adiabatic boundaries (Figure 2.10). Lastly, they calculated the average heat partition into the chip and the tool and the resulting temperature at the tool chip interface.

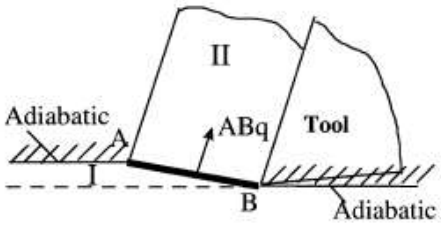

Figure 2.10 - Chao and Trigger's Model (1951) [17]

Although the model developed by Chao and Trigger provide a solution for the prediction of the average temperature of the shear plane, Chao and Trigger pointed out the difficulties that arise from the assumption that the heat flux is uniform at the tool chip interface, and concluded that to achieve the temperatures match on the two sides of the heat sources and to bring the two temperature distribution curves to near coincidence, is necessary to consider a non-uniform flux distribution [18]. In order to solve this problem, Chao and Trigger proposed an approximate analytical procedure in which the heat flux is assumed as an exponential function, although it gives a more realistic interface temperature distribution, this approach was time consuming. Alternatively, they developed a discrete numerical iterative method composed by the combination of analytical and numerical methods, which also includes the Jaeger's solution for the moving and stationary heat sources.

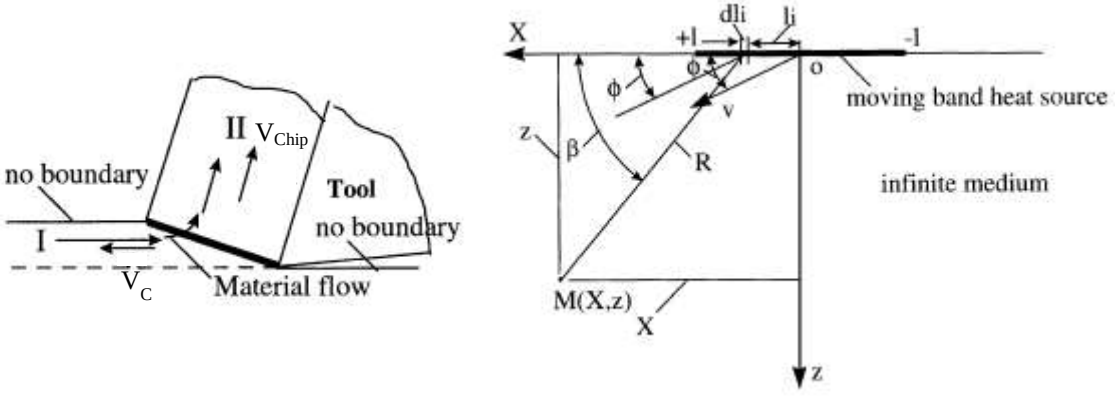

Figure 2.11 - a) Hahn's Model b) Schematic of Hahn's Model
Adapted from [17]

On the other hand, Hahn (1951) [17] developed an oblique moving band heat source model based on the chip formation process (Figure 2.11a). By considering the depth of the layer removed from the work material that passes continuously trough the shear plane, where is plastically deformed, to form the chip, the author established that the shear plane can be considered as a band heat source moving in the work material obliquely at the velocity of

cutting. Being the material on front and behind the heat source considered as a single body, the heat transfer by conduction and due to material flow are both considered.

According to Hahn's model (Figure 2.11b), the shear band heat source is considered infinitely long and having a 2l width, being the sum of infinitely small differential segments dl_i, and moving obliquely at an angle φ at a velocity V in an infinite medium. Thus, the solution for the temperature rise at a point M caused by the entire moving band in an infinite medium is given by [17]:

$$T_M = \frac{q}{2.\pi.\lambda_C} \int_{-l}^{+l} e^{\frac{-D.\cos(\xi-\varphi).V}{2.a_C}} . \; K_0 . \frac{R.V}{2.a_C} . dl_i \tag{2.22}$$

Where q is the heat liberation intensity of the heat source, a_C is the thermal diffusivity, λ_C is the thermal conductivity and K_0 is a Bessel function of the second kind and zero order [6].

Posteriorly, Chao and Trigger (1953) extended Hahn's model by considering a semi-infinite body (Figure 2.12) and assuming that the temperature at any point would be twice that for an infinite body, being this new model valid only for the special case in which the heat moving source is located on the boundary surface of an semi-infinite body [17].

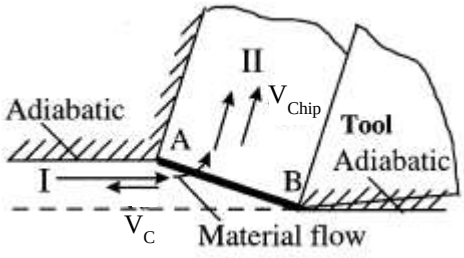

Figure 2.12 - Chao and Trigger's Model (1953)
Adapted from [17]

Komanduri and Hou (1999) [17] developed an analytical model for the temperature rise distribution in the work material and the chip due to the shear plane heat source, by modifying Hahn's moving oblique band heat source solution with the introduction of appropriate images sources for the shear plane. According to Komanduri and Hou [17], for continuous chip formation in orthogonal cutting, the shear plane heat source moves in a semi-infinite medium with the chip surface and the work surface being the boundaries of this semi-infinite medium, reason why the Hahn's oblique moving band heat source should be modified considering the boundaries effect and by using appropriate image sources. Thus, they considered that for an

adiabatic boundary, an image heat source (a mirror image of the original heat source with respect to the boundary surface) with the same heat liberation intensity should be considered, and determined the temperature rise distribution in the work material (Figure 2.13a) and the temperature rise distribution in the chip (Figure 2.13b).

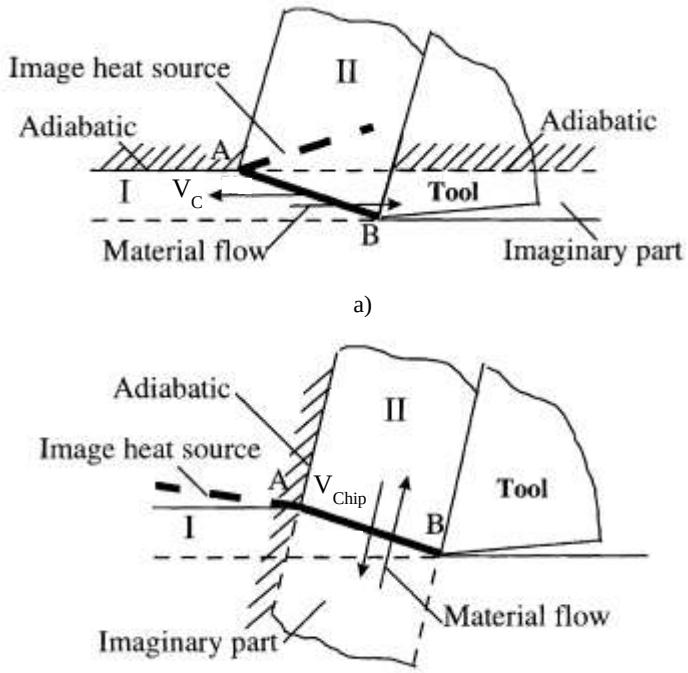

Figure 2.13 - Komandouri and Hou's Model (1999) for Thermal Analysis of a) Work material b) Chip
Adapted from [17]

In addition, Komandouri and Hou [19] determined the heat partition, the temperature rise distribution in the moving chip and the temperature rise in the stationary tool, due to the frictional heat source at the chip-tool interface. The authors developed an analytical model that uses a modified Jaeger's moving band heat source (in the chip) and a stationary rectangular heat source (in the tool), in which a non-uniform distribution of the heat partition along the chip-tool interface is considered with the purpose of matching the temperature distribution between the side of the chip and the side of the tool.

More recently, Praça (2014) [6] in his predictive analytical and numerical model for the orthogonal cutting process, based on Komanduri and Hou's investigations and extended the concept of non-uniform distribution of heat at the interfaces to encompass a set of contributions to the global temperature rise of the chip, tool and workpiece. The model further comprises a constitutive model for the material that is being cut, based on the work of Weber, a shear plane

model based on the Merchants model, a model that describes the friction contribution based on Zorev's model and a tool wear model based on Walford's work.

According to this work [6], the temperature rise at a point of the chip is given by the sum of the ambient temperature and the temperature rise due to the shear heat source and the friction heat source. With regard to the tool, when considering it perfectly sharp the author stated that the temperature rise at a point is given by the sum of the ambient temperature and the temperature rise due to the friction heat source and the induction heat source on the rake face, which is caused by the shear heat source. Also considering the tool perfectly sharp, the temperature rise in the workpiece was calculated as the sum of the ambient temperature and the temperature rise due to the shear heat source.

On the other hand, it was also considered the case in which the tool had wear flank and consequently its geometry was modified. In this case, the author considered that the temperature rise in a point of the workpiece had an additional rise of temperature due to the rubbing heat source. Similarly, the author also considered that the temperature rise in a point of the tool had an additional rise of temperature due to the rubbing heat source. Furthermore, the author considered that the temperature rise in a point of the tool had another contribution to temperature rise that was due to the induction heat source on the flank face caused by the shear heat source.

With the purpose of determine the state of the material being cut before calculating the temperature rise, Praça [6] developed a cycle to calculate the average temperature in the shear plane, comparing it to the temperature used to start the cycle (which is needed to input mechanical properties). This way, the cycle was computed until an admissible variation was found, and then the temperature rise in any point of the chip, tool and workpiece might be calculated.

2.4 Experimental Methods for Force and Temperature Measurements in Metal Cutting

In the metal cutting process several parameters affect the force components, such as the cutting speed, the feed rate and the depth of cut. The work of the force components applied on the tool is converted into heat, which is dissipated into the workpiece and the tool. Thus, the increase of forces on the tool implies more work requirements to remove material, which in turn originates

the temperature increase [20]. Different experimental methods have been developed for the evaluation of forces and temperatures in this area of research.

2.4.1 Force Measurement Methods

The cutting forces are extremely important because they allow the determination of machine power requirements and support loads, they possibly may cause the structural deflection of the workpiece, of the tool or of the machine, and also because they add energy that can result in excessive temperatures or unstable vibrations [21]. The measurement of cutting forces is the foundation of several models for predicting the cutting forces as function of different parameters such as the cutting velocity, feed rate, depth of cut, tool geometry or tool and workpiece materials. The measurement of cutting forces is usually done by using dynamometers that measure the deflections or strains in the elements that support the cutting tool, reason why the measurement instruments should have high rigidity and high natural frequencies. Thus, it is possible to guarantee the dimensional accuracy of the cutting and the minimization of vibration and chatter tendencies [9].

In metal cutting, the measurement of cutting forces began with the use of a variety of hydraulic, pneumatic, and strain gauge instruments [21]. More recently, piezoelectric dynamometers (employing quartz crystals) have been used. The piezoelectric dynamometers are appropriate for dynamics measurements, because they can be designed to have a higher natural frequency of vibration than other type of dynamometers [14].

2.4.2 Temperature Measurement Methods

The cutting temperatures are difficult to accurately measure when comparing to cutting forces, the temperature is a scalar field which varies along the system and is characterized in a determined region, while the cutting force is a simple vector characterized by three components [21]. On the other hand, the difficulties in temperature measurements also come from the metal cutting process itself, in which the small dimensions, the high speeds and the large temperature gradients have been challenging experimental investigation [22]. The measurement of temperature in metal cutting has a long history [5], and experimental works have been utilizing different measurement methods, based on various physical principles, to determine the temperature distribution, while new improvements have been developed in instrumentation. Among the different methods applied for temperature measurement in metal cutting the most

relevant are: thermocouple methods, radiation methods, thermal-sensitive paints methods and metallurgical methods.

2.4.2.1 Thermocouple Methods

The cutting temperatures are usually measured using thermocouple techniques [21]. A thermocouple works on the principle that two dissimilar metals joined together, forming two junctions, and maintained at two different temperatures (the hot and the cold junction) create an electromotive force across the junctions [23]. The electromotive force is dependent on the materials used for forming the thermocouple and on the temperature difference between the two junctions. According to Shaw [14], three principles of thermoelectric circuits, which are applicable in thermocouples, are the following:

- The electromotive force depends only on the temperature difference between the hot junction and cold junction, and is independent of temperature gradients along the system;
- The size and the resistance of the conductors do not influence the generation of the electromotive force;
- If the junction of two metals is at an uniform temperature, the electromotive force is not affected by the addition of a third metal, used two make the junction between the first two.

The thermocouple methods can be divided into the dynamic thermocouple technique and the embedded thermocouples technique. The dynamic thermocouple technique is one of the most widely used [9], [21]. In the dynamic thermocouple technique the tool and the workpiece are the elements of the thermocouple, allowing the evaluation of the average temperature at the tool-chip interface. The hot junction of the thermocouple is formed between the tool and workpiece interface, while the cold junction is formed in remote sections of the tool and the workpiece by electrical cables connections and this junction is maintained at constant temperature (Figure 2.14). So, to form a thermocouple the workpiece and the tool must be insulated from the surroundings. The dynamic thermocouple technique was applied by Shore, Gottwien and Herbert to measure the temperature along the face of the cutting tool [14].

However the dynamic thermocouple technique has some limitations, because the calibration of the thermocouple is critical to obtain accurate results and it can be found some difficulties to maintain the cold junction at constant temperature, especially when small tool inserts are used

[21]. The insulation requirements also create difficulties because the presence of insulating material may reduce the systems stiffness and lead to chatter at high velocities. Another relevant particularity is that the dynamic thermocouple technique do not allow studying the temperature distribution [9].

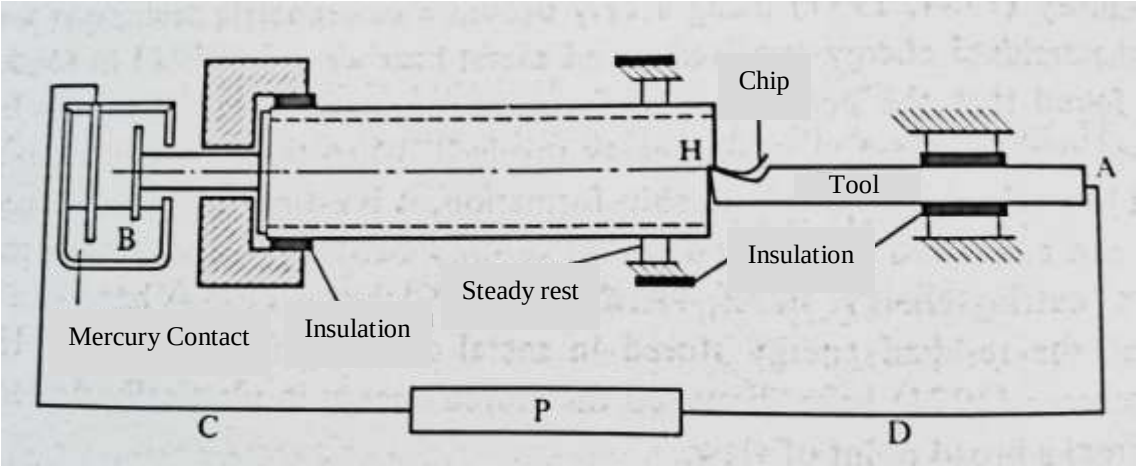

Figure 2.14 - Dynamic Thermocouple Technique
Adapted from [14]

On the other hand, in the embedded thermocouple technique the thermocouples are inserted in different locations in the interior of the tool (Figure 2.15), with some of them as close as possible to the surface [4]. With the use of many tools with thermocouples mounted on different points it is possible to map the temperature fields [14]. However, since the temperature gradients near the cutting zone are abrupt, the measurement accuracy depends on the thermocouples positioning. The measurement accuracy is also influenced by the thermocouples bead size, the thermal contact between the thermocouple and the specimen, and the influence that the holes (used to insert thermocouples) have on the temperature field. Nevertheless, the embedded thermocouple technique has been applied in orthogonal cutting [21].

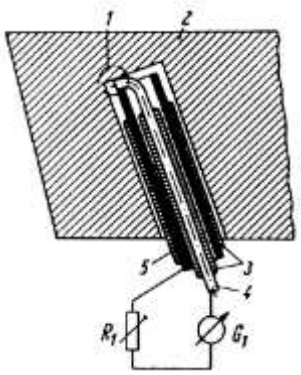

Figure 2.15 - Embedded Thermocouple Technique [4]

More recently with the growing evolution of technology it is possible to develop better instrumentation, as is the case of the work of Li et al. (2013) [13]. These authors developed an experimental setup in which the temperature distributions were measured by thin thermocouples embedded into the cutting insert (Figure 2.16) in the immediate surroundings of the tool chip interface, and on the other hand forces were measured by a dynamometer. In addition, the authors also measured the vibration by using an accelerometer. Figure 2.17 shows a schematic representation of the experimental setup and Figure 2.18 shows a real representation of the experimental setup.

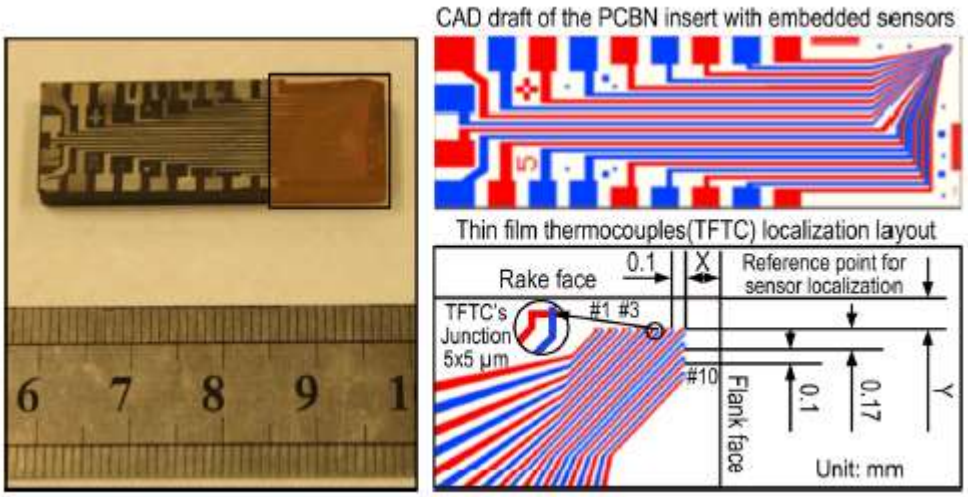

Figure 2.16 - Thin Thermocouples Embedded [13]

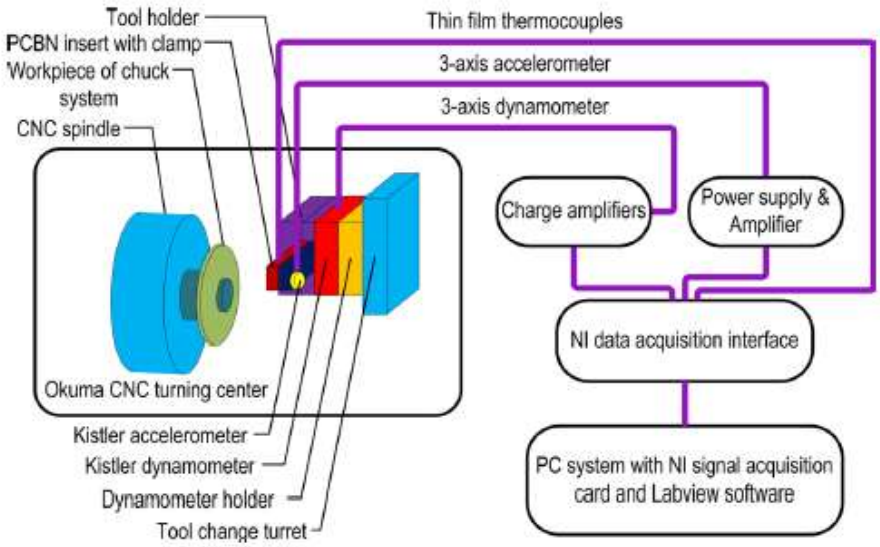

Figure 2.17 - Schematic Representation of the Experimental Setup [13]

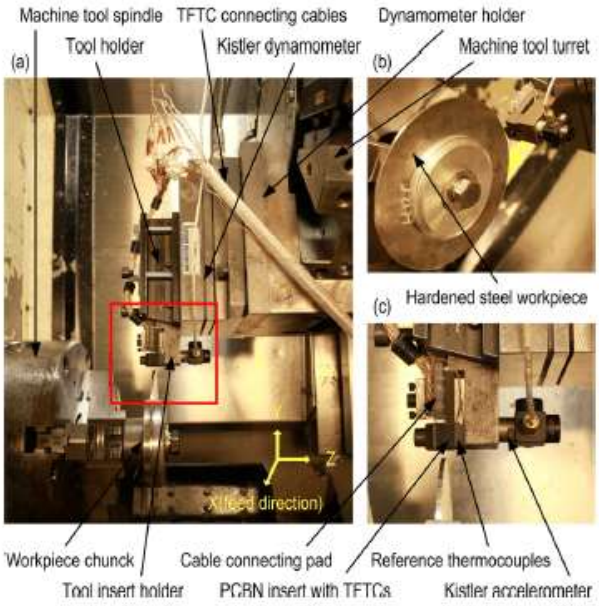

Figure 2.18 - Experimental Setup [13]

In this experimental setup the array of thin embedded thermocouples provided temperature measurements with a degree of spatial resolution of 100 µm and a dynamic response of 150 ns. The authors analyzed the steady-state and the dynamic response, as well as chip morphology and formation process based on the forces and temperatures variations evaluated by this experimental setup. They concluded that the temperature changes in the cutting zone depend on the shearing band location in the chip and the thermal transfer rate from the heat generation zone to the cutting tool. They also concluded that the chip formation morphology and the cutting temperature field distributions in the cutting zone of the cutting insert are both significantly affected by the material flow stress and by the shearing bands.

2.4.2.2 Radiation Methods

The cutting temperatures can be also determined by measuring the infrared radiation emitted by the cutting zone, when the tool-workpiece area can be directly observed [9]. In fact, the great advantage of the radiation methods is their non-intrusive characteristic. Instrumentation like pyrometers and thermographic cameras are used in this measuring method, in which the infrared radiation is detected and interpreted in terms of temperature [5]. These types of instrumentation usually require the estimation of the target emissivity, so that the measured infrared intensities can be converted in temperature. However, emissivity is difficult to determine because it depends on temperature and surface finish. Consequently, infrared measurements are difficult to perform with accuracy and often do not get similar results [9]. Besides, the temperature

measurement radiation methods are limited to exposed surfaces and cannot measure directly the temperature in bodies interior.

2.4.2.3 Thermal-sensitive Paints Method

Another method is the thermal-sensitive paints, in which the temperature distribution is estimated by coating the specimen with thermos-sensitive paints that change their color at known temperatures. This method is particularly useful to trace the isothermal lines [24]. The limitations of this method are the response time and accuracy for small temperature variations [24]. This method is also limited to accessible surfaces under steady conditions, and is not capable of giving accurate measurements at outworn surfaces [14]. Concluding, the thermal-sensitive paints method is suitable mainly for qualitative comparisons of temperature [21].

2.4.2.4 Metallurgical Method

The metallurgical methods are based on the principle that the metallic tool materials undergo metallurgical deformations or hardness changes which can be correlated to temperature. The structural changes can be determined performing a metallographic or microscopic examination, and since these changes provide an effective manner of determine the temperature, it is possible to map temperature distribution. On the other hand, micro hardness measurements can be performed on the tool after the cutting to determine temperature counters. The works published based on these techniques gave a clarification of tool temperature distributions and the location of the area of maximum temperatures [21]. Despite the structural changes has been used to study the temperature distributions in high-speed steel lathe tools, this technique of temperature estimation is limited to the range of cutting conditions suitable for high-speed steel and when high temperatures are involved [9]. Regarding the limitations of hardness changes technique, it is time-consuming and requires accurate hardness measurements [9].

2.4.2.5 Conclusion

In conclusion, each method has its own advantages and disadvantages. The appropriate method for measuring temperature in metal cutting truly depends on the situation under consideration and on different parameters, such as easy accessibility, accuracy needed, sensors size, cost of instrumentation, dynamics characteristics of the cutting process, and advancements on technology.

3 Methodologies and Experimental Procedures

In this chapter are presented the measurement methods and methodologies applied in the experimental investigation, and the equipment used, as well as the monitoring system for data acquisition. The chapter also describes the experimental procedures, such as the production of specimens and auxiliary components.

3.1 Adopted Measurement Methods

Since the experimental investigation is restricted by the equipment available on the mechanical technology laboratory, the adopted orthogonal configuration is the one in which the workpiece is clamped in a mandrel and the tool moves perpendicular to the mandrel rotation axis with the cutting edge parallel to this axis, in a lathe.

The alternative configurations, presented on the state of the art, are not a suitable solution for the problem under study, because the configuration with a long tube is limited by the maximum length of the lathe, which do not provide enough space to perform the experiments, while the quick and stop device even adapted to perform continuous tests do not allow to evaluate the temperature rise due to the short duration of the experiment, resulting from the short course of the available shaper.

On the other hand, the temperature measurement method applied in this investigation is restricted by the available methods (on the laboratory) and also by the type of measurement desired. Since it is intended to make a continuous measurement of the temperature at different points, in order to analyze the temperature rise, the embedded thermocouple technique is the chosen solution. With respect to the force measurement method, it is adopted the use of a piezoelectric dynamometer because it is widely used at forces evaluation, in metal cutting research. Thus, with the available technology and available instrumentation will be developed an experimental setup intended to be similar to the on developed by Li et al. (2013) [13].

Taking into account the temperature and forces measurement methods chosen, it is possible to proceed with the implementation and evaluation of the experimental setup.

3.2 Specimens Production

To evaluate the performance of the experimental setup were produced thin discs, cutting inserts and insulating plates. The thin discs were produced from the materials presented in Table 3.1, and its geometries and dimensions are presented in the Appendix.

Table 3.1 - Materials Used in the Construction of the Thin Discs

Material	Designation
Construction Alloy Steel	EURONORM 42 Cr Mo 4
Stainless Steel	AISI 304 L
Low Carbon Steel	AISI 1020

The specimens of stainless steel and construction alloy steel were produced from rods laminated perpendicularly to the direction in which the orthogonal cutting tests were performed, while the specimens of low carbon steel were produced from sheet, which had the lamination plane coincident with the orthogonal cutting plane of the cutting tests. The specimens of stainless steel and construction alloy steel were produced on a conventional lathe (Figure 3.1), and the specimens of low carbon steel were cut by laser technology. Nevertheless, all the specimens of thin discs had the same dimensions, having an outside diameter of 200 mm and a width of 3 mm.

Figure 3.1 - Specimens of Stainless Steel and Alloy Steel Production

In respect to the cutting inserts, they were produced in tungsten carbide taking into account the variety of materials selected for the thin discs specimens, and also the fact that the temperature measurement technique chosen imposed the use of a non-coated tool. The cutting inserts were made by Duryt and its characteristics are presented in Table 3.2.

Table 3.2 - Properties of the Tungsten Carbide Used in Production of the Cutting Inserts

Properties	Classification
Binder Content & Percentage	Cobalt (Co) 5.5%
Hardness	91.5 HRA
Grain Size	1.2 µm

Concerning to the tool geometry, the cutting inserts were all produced with a 4 mm width and maximum dimensions between the broadsides of lateral faces of 16 mm. The clearance angle chosen was the same for all the cutting inserts, while three different values were chosen for the rake angle. The selected angles and the cutting insert classification are presented in Table 3.3.

Table 3.3 - Cutting Insert Classification and Selected Angles

Cutting Insert	Rake Angle (º)	Clearance Angle (º)
Type I	0	3
Type II	5	3
Type III	10	3

Detailed information of the cutting inserts dimensions and geometry are presented in Appendix. In Figure 3.2 are shown the cutting inserts, where can be observed its geometries and the different angles. It should be noted that the cutting inserts of type II and type III have a slightly curved shape at the end of the rake face. The curved shape was created with the purpose of facilitate the chip flow.

a) b) c) d)

Figure 3.2 - Cutting Inserts: a) Type I b) Type II c) Type III d) Cutting Inserts Side by Side

The insulating plates were produced with two different materials (Celeron and Zirconia) and had the same geometries and dimensions of the cutting inserts. These insulating plates were built with holes near the tip (Figure 3.3a), which were made with a drill of 1 mm diameter. In

the back side of the insulating plates, that is the plate side that is pushed against the tool holder, was built a central slot that allows the thermocouples to be driven up to the holes (Figure 3.3b).

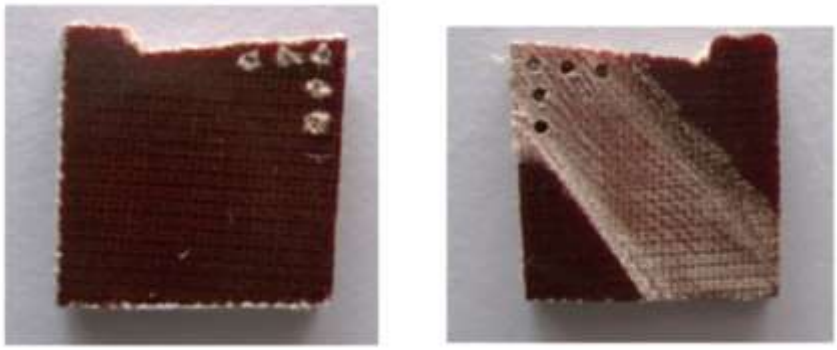

a) b)

Figure 3.3 - Insulating Plates of Celeron: a) Front Side or Tool Side Face b) Back Side or Tool Holder Face

3.3 Auxiliary Components Production

In the present work were designed and constructed several auxiliary components, including an assembly system for the thin discs, a support to fix the dynamometer on the tool turret of the CNC lathe and a tool holder specially developed for the chosen temperature measurement technique. The assembly system of the thin discs is composed by a mandrel (Figure 3.4a), a pin (Figure 3.4b), a washer (Figure 3.4c) and a nut (Figure 3.4d).

a) b)

c) d)

Figure 3.4 - Assembly System of Thin Discs: a) Mandrel b) Pin c) Washer d) Nut

In the assembly system, the thin discs are mounted in the mandrel and pushed against the washer by the clamping action produced by the tightening of the nut onto the threaded end of the mandrel (Figure 3.5). To prevent the unscrewing of the nut and the slipping of the thin discs between the mandrel and the washer, was produced a pin that crosses trough the washer and the thin disc up to the blind hole existing on the mandrel. The pin blocks the rotation between the elements. The drawings and dimensions of the components of the assembly system are in the Appendix.

Figure 3.5 - Assembly System Assembled with a Thin Disc

With regard to the support to fix the dynamometer on the tool turret, it was built due to be impossible the direct assembly between these two components (Figure 3.6a). The support is constituted by two components, which are assembled between them, and does the fixing connection between the dynamometer and the turret (Figure 3.6b and Figure 3.6c). The components that constitute the support were produced with high parallelism between faces in order to ensure the geometrical conditions of orthogonal cutting. Their drawings and dimensions are in the Appendix.

a) b) c)

Figure 3.6 - Tool Turret: a) Empty b) Assembled With the Fixing Support c) Assembled With the Fixing Support and the Dynamometer

Lastly, the tool holder was designed in order to be assembled directly to the dynamometer (Figure 3.7a). The tool holder was produced with a slot in its backside (Figure 3.7b and Figure 3.7c), which enables the passage of the thermocouples up to the holes and thence to the lateral face of the cutting insert through the insulating plates. The attachment of the cutting insert and the insulating plate in the tool holder is done by a side support (Figure 3.7d). The drawings and dimensions of the tool holder are in the Appendix.

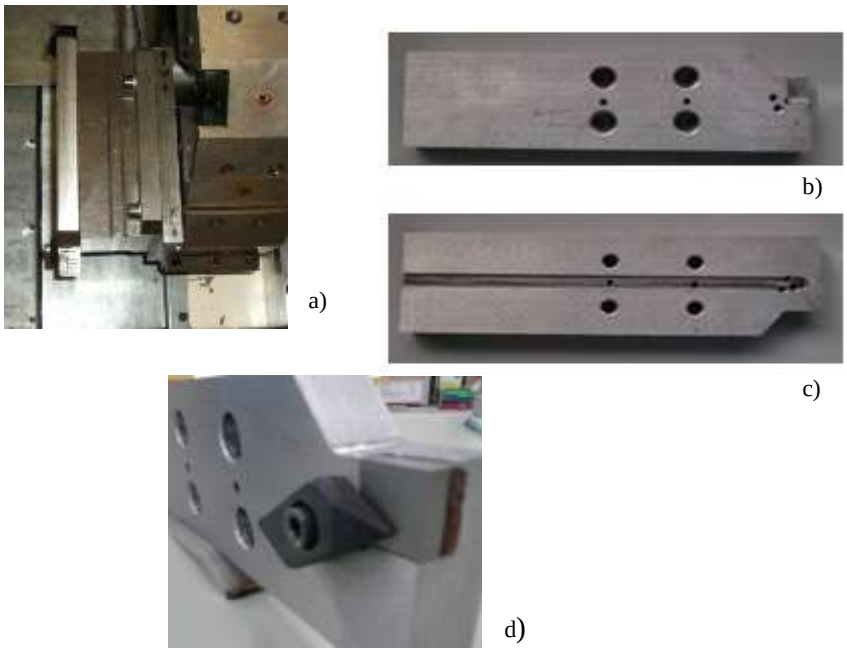

Figure 3.7 - Tool Holder: a) Assembled in the Dynamometer b) Front Side c) Back Side d) Assembly of the Cutting Insert and the Insulating Plate by the Side Support

3.4 Equipment

The orthogonal cutting tests were carried out in a LEADWELL LTC-10 APX CNC lathe available in the laboratory and presented on Figure 3.8.

The monitoring and data acquisition of the forces were performed by a Kislter dynamometer (Figure 3.9a), model 9257B, which was connected to a multi channel charge amplifier Kilster 5070 (Figure 3.9b).

Figure 3.8 - CNC Lathe

a) b)

Figure 3.9 - Kistler: a) Dynamometer b) Amplifier

Regarding to the temperature measurements, they were performed with thermocouples of type K insulated with a PTFE (Polytetrafluoroethylene) cable. The diameter of the sensors was 0.6 mm and the length was 1000 mm [25]. Since the length of the thermocouples was not long enough to directly connect them to the data acquisition module, copper multi-wired cables were used for making the connections. In Table 3.4 are presented the maximum and minimum temperatures of the thermocouple temperature range, as well as the accuracy of the thermocouple. Despite the operating temperature of thermocouples was between -50 ºC and 260 ºC and the cutting temperatures were higher, the insulating cable integrity was maintained because only the tip of the thermocouple was in contact with the cutting insert.

Table 3.4 - Thermocouples Specifications Adapted from [25]

Properties	Classification
Maximum Temperature of the Temperature Range	+1100
Minimum Temperature of the Temperature Range	-50º
Accuracy	±1.5º

The conversion of the analog signals of forces and temperatures into digital signals was performed by the acquisition data system NI cDAQ -9178 (Figure 3.10).

Figure 3.10 - Acquisition Data System

The signals were processed and the data corresponding to the measured values were presented in LabVIEW software (Figure 3.11).

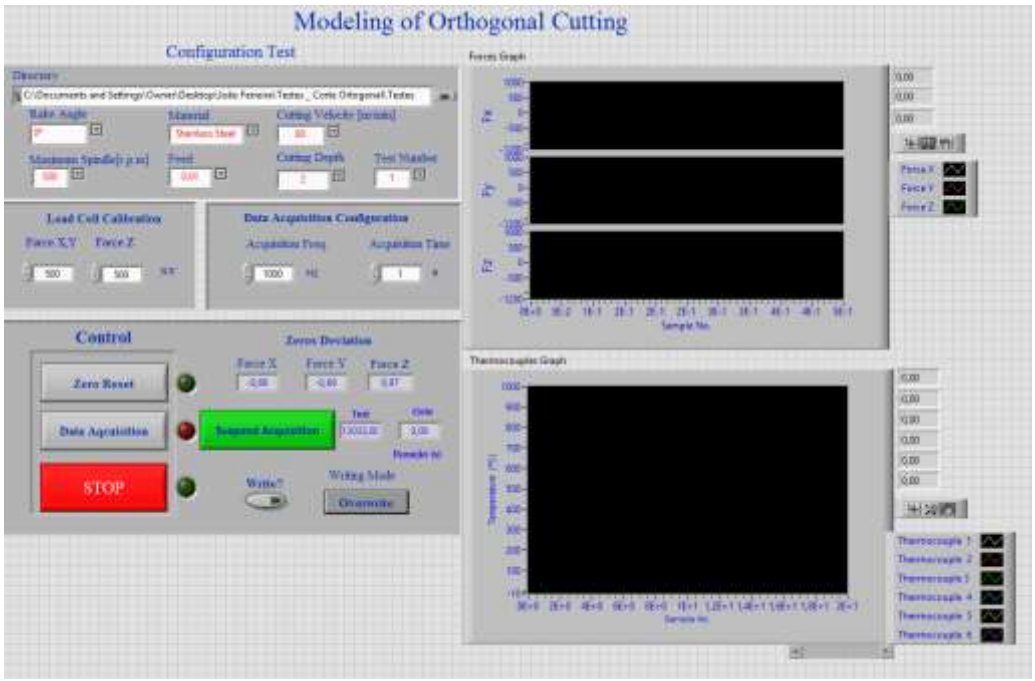

Figure 3.11 - Data Acquisition Program – LabVIEW

A hot air gun was used to perform the heating of the cutting insert in the preheated experimental tests. In addition, the assembly system of thin discs, the fixing support of the dynamometer and the tool holder, presented in section 3.3, were used.

3.5 Implementation of Temperature and Forces Measurement Methods

In the implementation of the forces measurement method was adopted only one technique, which was the assembling of the tool holder directly in the dynamometer to evaluate the cutting force (Figure 3.12), the thrust force and the passive force that is perpendicular to the orthogonal cutting plane.

Figure 3.12 - Implementation of Forces Measurement Technique

On the other hand, for the implementation of the temperature measurement method three different techniques were adopted in order to comprehend which solution works best for a correct reading of the thermocouples. The attachment of the thermocouples was an important aspect that influences the measurement and positioning of the thermocouples, but was restricted by the available space. In the implementation of temperature measurement techniques was defined the placement of the thermocouples between a side face of the cutting insert and an insulating plate. The insulating plane has the function of do not allow the heat to flow directly from the cutting insert to the tool holder, thus enabling a correct temperature measurement.

To carry out the placement of thermocouples was necessary to make some adaptations to the thermocouples (Figure 3.13). The insulating parts of insulation cables near the hot junction of the thermocouples were stripped, resulting in the exposure of the thermocouples metal wires which had a 0.2 mm. In order to guarantee the electrical insulation of the metal wires, these were covered with an electrical insulating varnish, while the hot junction remained uninsulated.

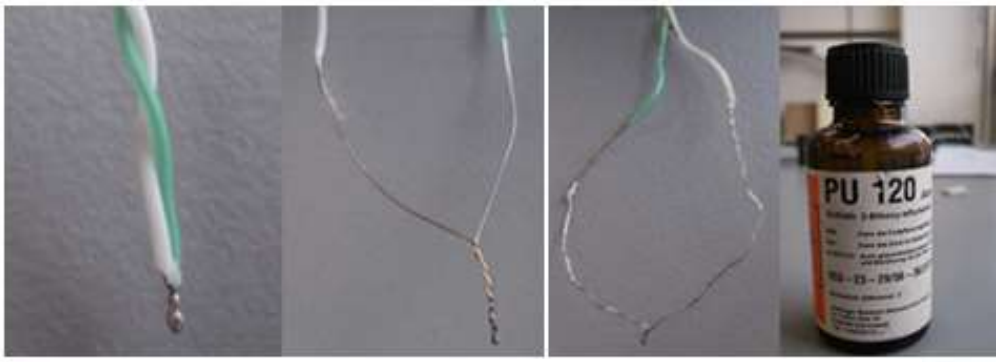

a) b) c) d)

Figure 3.13 - Thermocouples Adaptations: a) Original Thermocouple b) Stripped Thermocouple c) Varnished thermocouple d) Varnish

Three different solutions were implemented in the thermocouples attachment. In the first solution, the thermocouples were attached by mounting the tip of the thermocouples inside the insulating plate holes (Figure 3.14a) and placing the tips against the side face of the cutting insert (Figure 3.14b). Then the cutting insert and the thermocouples were placed in the tool holder, and lastly the side support was tightened (Figure 3.14c) enabling the thermocouples attachment.

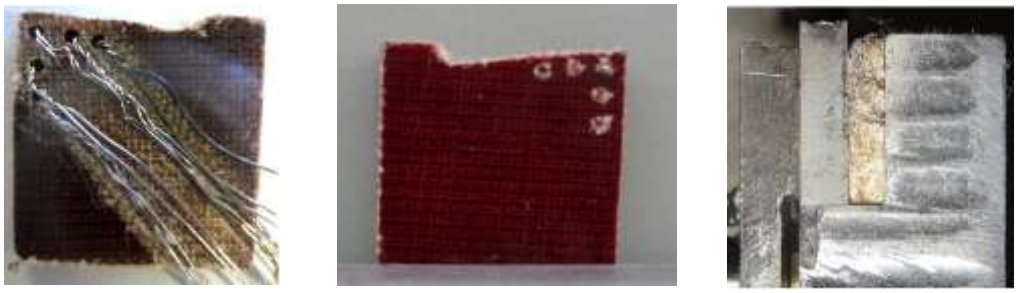

a) b) c)

Figure 3.14 - Thermocouples Attachment: a) Mounting the Tips of Thermocouples b) Placing the Tips of Thermocouples c) Assembly in the Tool Holder

In this solution, the insulating plate had also the function of ensure the positioning of the thermocouples. The maximum number of thermocouples that was possible to use in this solution was limited to five, due to the size of the side face of the cutting insert and the diameter size of the sensors. In Figure 3.15 is shown the thermocouples positioning.

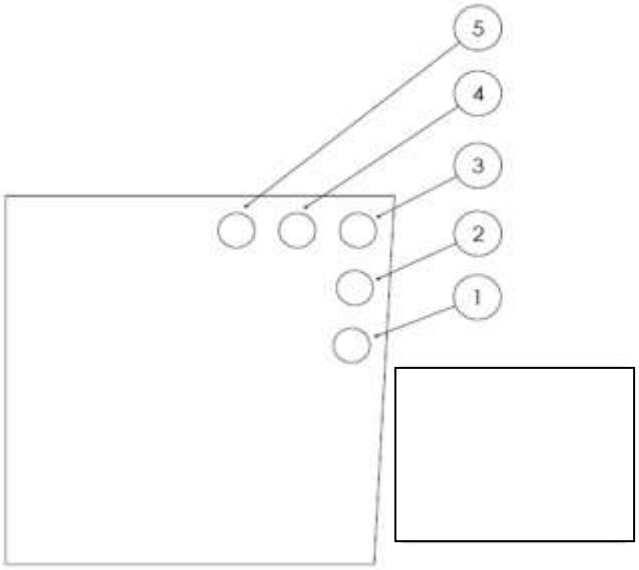

Figure 3.15 - Placement of the Thermocouples in the Insulating Plate

To ensure a better thermal contact between the cutting insert and the thermocouples was used a thermal paste between the face of the cutting insert and the insulating plate, where the thermocouples were embedded. Alternatively, anticipating a less good performance of thermal paste to perform the thermal contact it was implemented a second solution with a cooper plate (Figure 3.16) with 0.5 mm between the cutting insert and the insulating plate. Thus, the thermal contact was made between the cutting insert and the cooper plate, where the thermocouples were embedded. In this solution were only used two thermocouples, the third and the fifth thermocouples.

Figure 3.16 - 3rd Thermocouple Mounted on the Cooper Plate

However, by making a preliminary theoretical evaluation of these two first solutions, it was possible to understand that vibrations during cutting process might cause poor contact between the thermocouples and the cutting insert. Therefore a third solution was implemented in order to

attach the thermocouples. In this solution the thermocouples were brazed directly in the cutting insert (Figure 3.17) and attached against the insulation plate in the tool holder. The type of brazing applied was silver brazing and it was performed using a blowtorch. As a result of the thermocouples dimensions, the cutting insert dimensions and the type of brazing applied the positioning of the thermocouples was performed as close as possible to the tip of the cutting edge, but without positioning accuracy. The maximum number of thermocouples used in this solution was two.

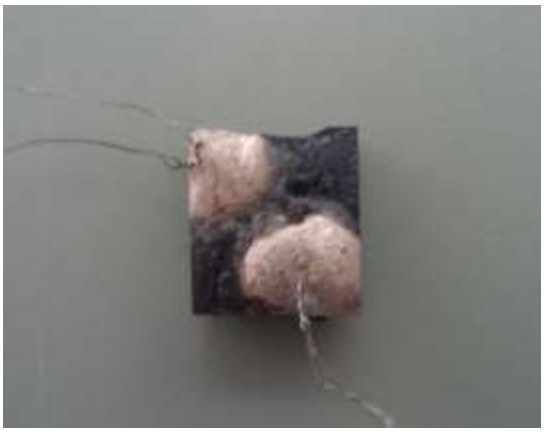

Figure 3.17 - Thermocouples Brazed in the Cutting Insert

This solution was based on the foundation that the insertion of an intermediate metal in the hot junction does not affect the output voltage, provided the two junctions formed by the insertion are maintained at the same temperature [23]. The brazing was performed in order to obtain a point, however it was obtained a brazed area instead. Therefore the temperature measurement do not represent the temperature of a point, instead it represents the mean temperature of the brazed area where the thermocouple was brazed. Furthermore, there was no guarantee of an accurate positioning of the thermocouple.

3.6 Cutting Parameters and Test Conditions

Different cutting parameters and test conditions were applied to evaluate the performance of the temperature and forces measurement techniques implemented in the experimental setup. The feed velocity and the cutting velocity were both limited by the CNC lathe. Regarding to the cutting velocity, the tests were performed with a constant cutting velocity of 100 meters per minute. Considering the feed velocity, different feeds were used in the range between 0.01 mm per revolution and 0.1 mm per revolution. The duration of the tests was determined by the relation between the cutting velocity, the feed velocity and the depth of cut. The cutting depth varied between 10 mm and 40 mm in diametric dimensions, once the tests must be short

because the heat might have difficulties to flow out of the thin disc. The cutting width was constant and equal to 3 mm. Besides, different materials and different cutting insert angles were used in the tests. In Table 3.5 are shown the cutting parameters and test conditions of the tests performed in the experimental setup.

Table 3.5 - Matrix of Cutting Parameters and Test Conditions

Cutting Velocity (m/s)	**Temperature Technique**	**Rake Angle (º)**	**Material of Thin Discs**	**Feed Velocity (mm/rev)**	**Depth of Cut (mm)**	**Width of Cut (mm)**
100	Thermocouple Embedded in Thermal Paste	0	Low Carbon Steel	0.01	10	3
100	Thermocouple Embedded in Cooper Plate	10	Construction Alloy Steel	0.02	40	3
100	Thermocouple Embedded in Cooper Plate	0	Construction Alloy Steel	0.02	40	3
100	Thermocouple Brazed in the Cutting Insert	5	Stainless Steel	0.1	40	3

In Figure 3.18 is shown an example of one of the tests carried out.

Figure 3.18 - Example of the Test Performed

Additionally, pre-tests were conducted prior to performing each test, to assure a good contact between the thermocouples and cutting insert. By using a hot air gun to heat the cutting insert, the temperature at the cutting insert increased and it was verified if the thermocouples detected the temperature increase. Thus, it was possible to conclude if the thermocouples were prepared or not to perform the tests.

Concerning to the initial temperature of the cutting insert, the tests were performed with two different initial conditions. Some of the tests were performed with the cutting insert initial temperature equal to the ambient temperature, while in the remaining of the experimental tests the cutting insert was pre heated up to 200º C. The pre heated tests had the purpose of evaluating the evolution of the temperature over a range of temperatures exceeding those that would be achieved if the initial temperature of the cutting insert was at ambient temperature, once the tests had a short duration.

4 Results and Discussion

The results obtained in the experimental part of this dissertation will be presented and discussed in this chapter. Will be evaluated the performances of the temperature measurement techniques and of the forces measurement technique implemented. Since three different temperature measurement techniques were implemented for the thermocouples attachment, the chapter is divided in three parts: tests performed with thermocouples embedded in thermal paste; tests performed with thermocouples embedded in cooper plate; tests performed with thermocouples brazed in the cutting insert.

4.1 Tests Performed with Thermocouples Embedded in Thermal Paste

In the tests performed with thermocouples embedded in thermal paste were used thin discs of low carbon steel and insulating plates of Celeron. The number of thermocouples used to evaluate the temperature in the tests was five. The cutting inserts used in these tests had a rake angle of 0º degrees, the cutting velocity was 100 meters per minute, the feed was 0.01 mm per revolution and the cutting depth was 10 mm. In the following figures are presented the forces and temperatures measured in two different tests performed with the conditions and materials mentioned above.

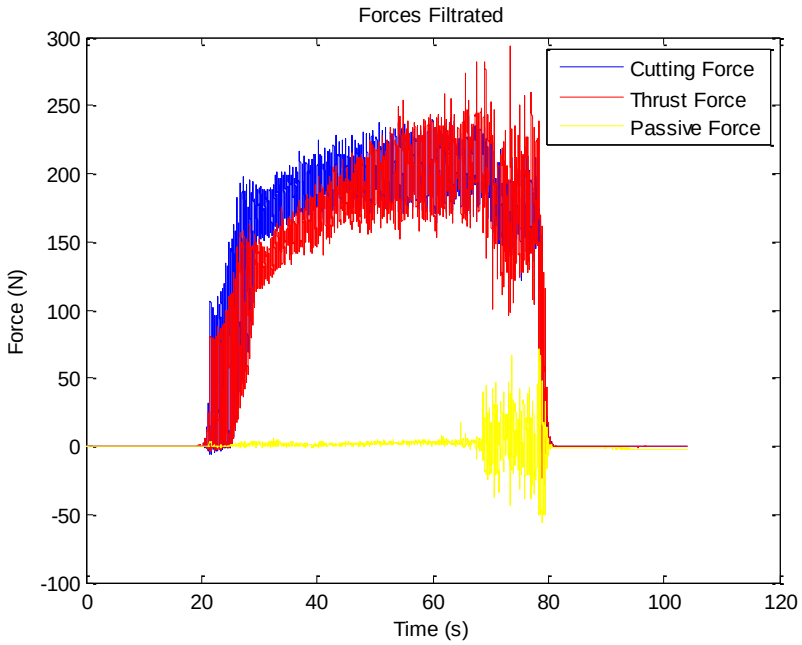

Figure 4.1 - Forces Measurement: Embedded Thermocouples (Thermal Paste) - Unfinished test

In Figure 4.1 and Figure 4.2 are presented the forces and temperatures measured in the first test, which was not carried out until the end because of the occurrence of excessive vibration in the middle of the test. In Figure 4.1 can be seen that the vibration phenomenon aroused around the seventy second, where the cutting force graph, the thrust force graph and passive force graph show the onset of vibration. Although the test was not completed it is possible to obtain relevant information from the results. As expected the passive force is almost zero, in conformity with the orthogonal cutting assumptions. On the other hand, the cutting force and the thrust force have a good agreement, with the cutting force values measured being higher than the thrust force values measured.

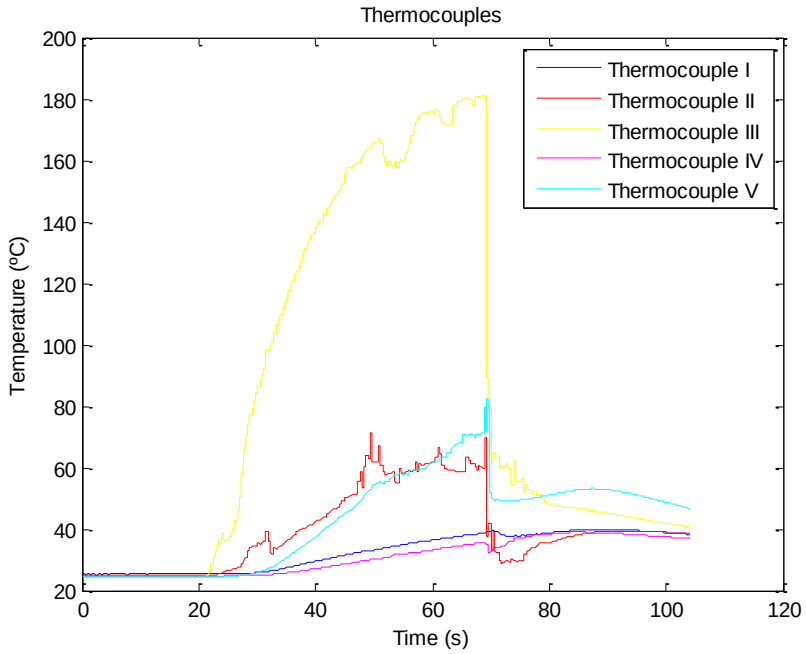

Figure 4.2 - Temperatures Measurement: Embedded Thermocouples (Thermal Paste) – Unfinished test

Regarding to the temperature measurement results, they are very low and do not correspond to the effective temperatures that were developed in the cutting insert. Besides, it was expected that the temperatures gradually diminish as the distance to the cutting edge increases, and in Figure 4.2 can be observed that the fifth thermocouple, which is more farther from the cutting edge than fourth thermocouple, has a higher temperature. The graphic also shows the influence of vibration in the temperature measurement. At the moment that vibration begins the readings immediately have lower values of temperature. In addition, it is possible to identify in the graphics of the second and the third thermocouples some time periods (before the vibration phenomenon) where the elevation of temperature decreases rather than increasing. Nonetheless the decreasing of temperature during the cutting does not provide a correct representation of the thermodynamics of cutting. These results evidence the poor contact between the thermocouples

and the side face of the cutting insert promoted by the thermal paste when vibrations takes place.

The second test was performed completely without interruption. The test exhibited a continuous phenomenon of vibration similar to the one that happened in the previous test, but in this second test, the phenomenon took place throughout the test. In Figure 4.3 is possible to see the increased vibration in the graphic of the passive force, around the forty fifth second. It can be observed that the cutting force and the thrust force mean values do not differ from the values of the previous test as expected. With regard to the passive force, although the mean value of the passive force is almost zero like in the first test, the passive force signal has a continuous noise due to the continuous vibration phenomenon.

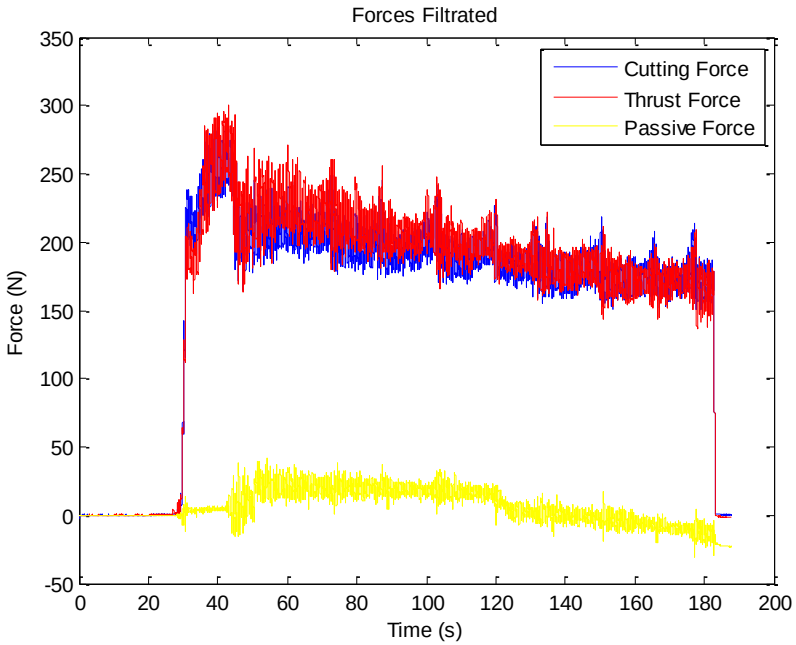

Figure 4.3 - Forces Measurement: Embedded Thermocouples (Thermal Paste)

Similarly to the first test, the second test also showed inaccurate temperature measurement results. In Figure 4.4 is possible to observe the effect of the vibration phenomenon on the thermocouples measurement. It is possible to identify in the graphics of the thermocouples several nearly instantaneous increases and decreases of temperatures due to vibration, despite the graphics of the thermocouples shows a growing trend of temperature during the test. A prime example of the vibration effect is the graphic of the third thermocouple that has a nearly instantaneous discontinuity of temperature around the forty fifth second. At this moment the temperature rises instantaneously to approximately 150º C and then abruptly decreases about 100º. After that, the measured temperature progressively increases until the end of the test is

reached. Regarding to temperatures distribution, in Figure 4.4 can be observed that some of the temperature measurements of thermocouples more distant from the cutting edge have higher temperatures than closer ones, as is the case of the second thermocouple and the first thermocouple, contrary to what was expected. Concluding, the results obtained in the second test reinforce the evidence of bad contact of the thermocouples embedded in thermal paste.

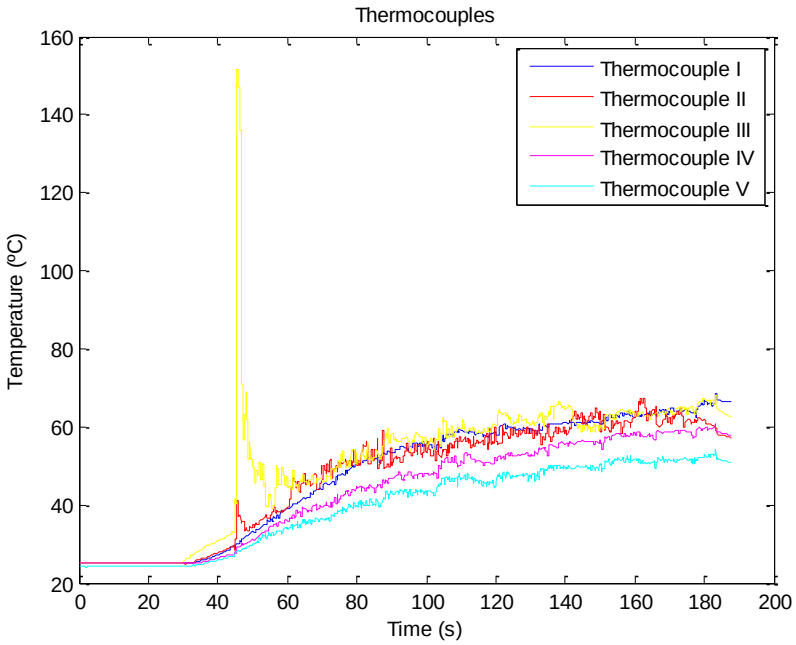

Figure 4.4 - Temperatures Measurement: Embedded Thermocouples (Thermal Paste)

4.2 Tests Performed with Thermocouples Embedded in Cooper Plates

In the tests performed with thermocouples embedded in cooper plates were used thin discs of construction alloy steel and insulating plates of Zirconia. The number of thermocouples used to evaluate the temperature in the tests was two. The thermocouples that performed the readings were the third thermocouple and fifth thermocouple. The cutting velocity was 100 meters per minute and the feed was 0.02 mm per revolution. A cutting insert with a 10º rake angle was used and the cutting depth was 40 mm in diameter. The test was performed with pre heating of the cutting insert to 200 ºC.

Figure 4.5 and Figure 4.6 represent the forces and temperatures measurements, respectively, of the test performed. As expected, similarly to the previous tests the cutting force is higher than the thrust force. However, the passive force graphic unexpectedly does not follow the trend of a horizontal straight line that passes close to null values. Instead, it shows a tendency towards negative values which mean the existence of compression of the tool holder against the tool

turret. Perhaps this tendency relates to the misalignment of the cutting insert in this test in particular, since it was not observed in the remaining tests. In addition, the result also shows the existence of the vibration phenomenon in the direction perpendicular to the cutting plane.

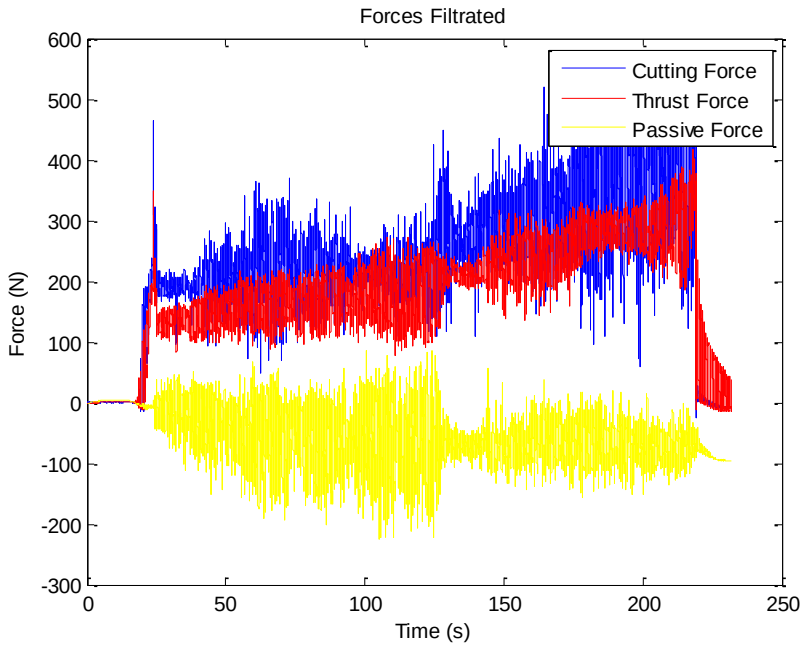

Figure 4.5 - Forces Measurement: Embedded Thermocouples (Cooper Plate) - Rake Angle 10º

Regarding to the temperature measurements (Figure 4.6), can be seen that at the time the test is initiated the temperatures measured by the two thermocouples do not differ among themselves. However the values of the temperatures measured at the beginning of the test do not correspond to the pre heating temperature value. This temperature difference is associated to the time interval that happens between the end of the pre heating and the beginning of the test, and therefore this result was expected.

At the moment the test begins, around the twentieth fifth second, is evident the temperature rise in both thermocouples, it is possible to conclude that both thermocouples are in contact with the cutting insert. However, after the beginning of the test the fifth thermocouple presents poor contact. Indeed, around the hundred thirtieth second the value of the temperature measured by the fifth thermocouple suddenly decreases. It should be noted that at this precise moment, in Figure 4.5 is possible to observe a decrease in the noise signal of the forces. This result shows the influence of the vibration phenomenon in the thermocouples embedded in cooper plate solution. In contrast, the temperatures measured by the third thermocouple exhibit a continuous increase as expected.

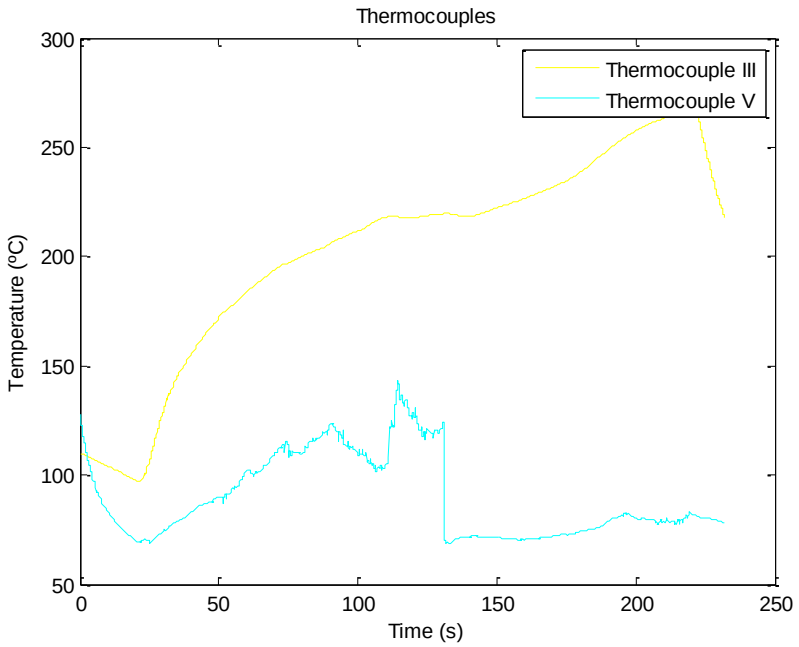

Figure 4.6 - Temperature Measurement: Embedded Thermocouples (Cooper Plate) - Rake Angle 10º

In addition, another test was performed in which the only difference from the previous test was the rake angle of the cutting insert. In this second test the rake angle was 0º. During the test the chip turned incandescent and the forces increased unexpectedly, reason why it was not carried out till the end. This test deserves special attention because during the test the cutting insert became completely destroyed and the thin disc became partially hardened.

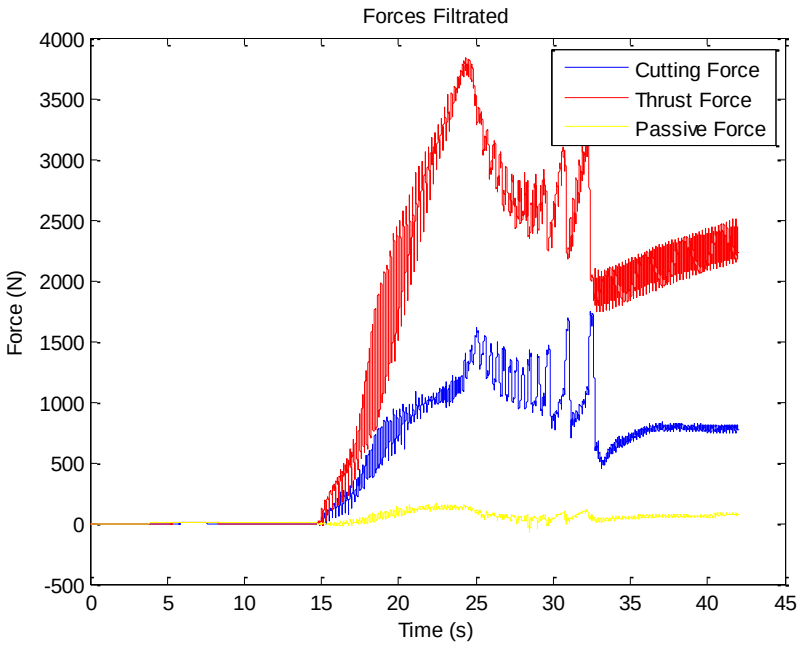

Figure 4.7 - Forces Measurement: Embedded Thermocouples (Cooper Plate) - Rake Angle 0º

In Figure 4.7 can be seen that from the beginning of the test the thrust force is higher than the cutting force, evidencing the difficulty in performing the material cutting. Besides, the graphics of cutting force and thrust force show a tendency of increase on both forces up to the twentieth fifth second. Then the graphics show a decrease and at the thirty third second, when the cutting was stopped, the feed force increases and the cutting force becomes constant. On the other hand, the passive force takes values near zero as expected.

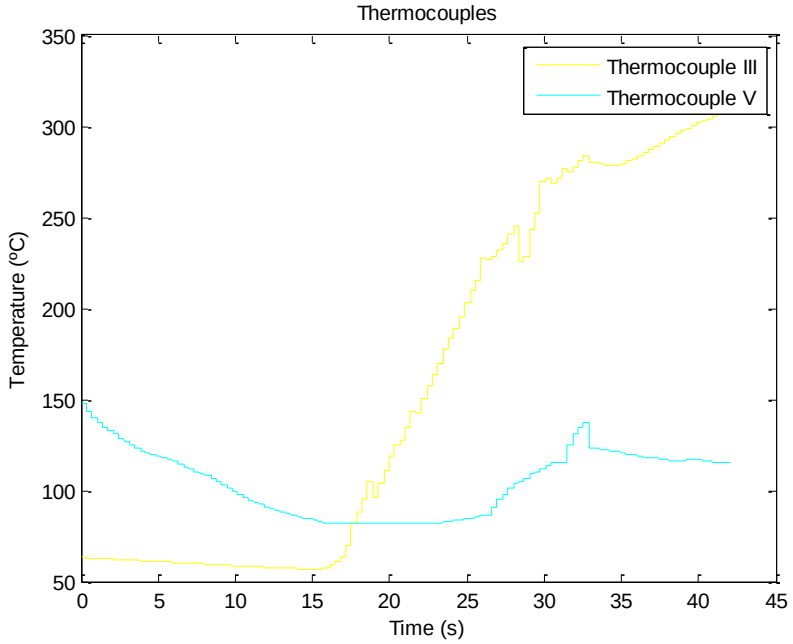

Figure 4.8 - Temperature Measurement: Embedded Thermocouples (Cooper Plate) - Rake Angle 0º

Regarding to the temperature measurements, the cutting insert was pre heated however the thermocouples readings do not show similar initial temperature (Figure 4.8). This result shows that the cutting insert was not uniformly heated. Further, the temperature measurements performed by the third thermocouple shows a continuous growth throughout the test, while the temperature measurements of the fifth thermocouple only start to grow at the time corresponding to the decrease of both forces. However, the third thermocouple shows an unexpected result that is the measurement of increasing temperatures in the period after the test is stopped, during which the fifth thermocouples starts to read a slowly decrease of temperature. Since when the test was stopped the only body in contact with the cutting insert that could be at higher temperature than the cutting insert was the thin disc, and combining this fact to the increasing temperatures read by the third thermocouple after the test was stopped and the hardened surface of the thin disc in the end of test, it can be concluded the lack of capacity of the disk to flow out the heat accumulated during the test. In Figure 4.9 is shown the thin disc that was hardened during the realization of this test.

Figure 4.9 - Hardened Disc

4.3 Tests Performed with Thermocouples Brazed in the Cutting Insert

In the tests performed with thermocouples brazed in the cutting insert were used thin discs of stainless steel. The insulating plates were made of Zirconia. The number of thermocouples used to evaluate the temperature in the tests was two. The thermocouples that performed the readings were positioned as close as possible to the cutting tip. Wherein the first thermocouple was closer to the cutting edge and the second was more distant. These tests were also performed with pre heating of the cutting insert to 200 ºC. The cutting velocity was 100 meters per minute and the feed was 0.1 mm per revolution. A cutting insert with a 5º rake angle was used and the cutting depth was 40 mm in diameter.

As expected, in Figure 4.10 can be seen that the cutting force is higher than the thrust force and the passive force is almost zero. Furthermore, it is possible to identify that the results obtained have noise, resulting from the vibration phenomenon that occurs during the cutting.

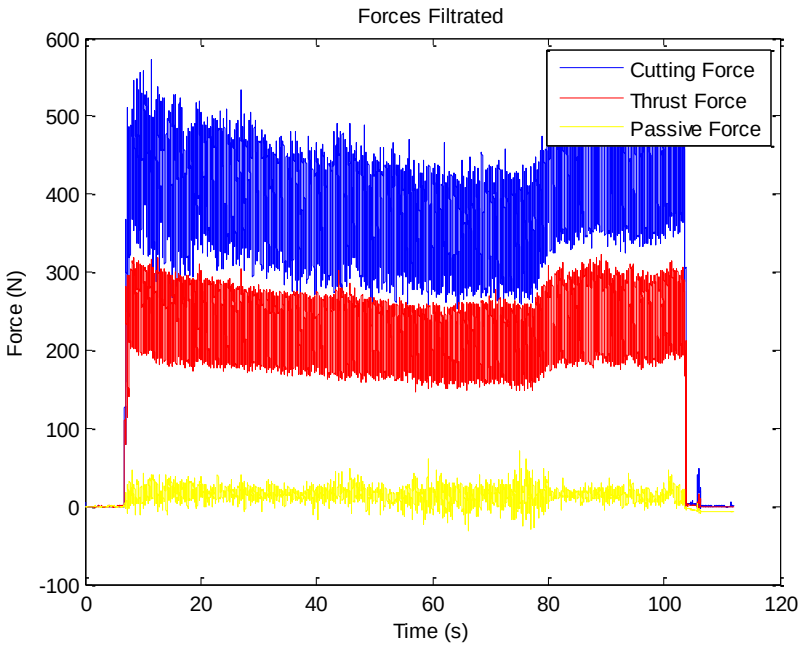

Figure 4.10 - Forces Measurement: Brazed Thermocouples

Regarding to the evaluation of temperature, in Figure 4.11 can be seen that the initial temperatures measured by the two thermocouples are approximately 30 ºC. These initial values of temperature do not match with the temperature of pre heating of the cutting insert, and this difference is a result of a long time interval between the end of the pre heating and the beginning of the test. Thereafter, the pre heating done to the cutting insert turns out to be insignificant.

Besides, in the graphics can be seen that the thermocouples did a correct reading of the temperature during the test, by describing a temperature increase during the test and then a temperature decrease after the test is finished. In the beginning of the test the second thermocouple reads higher temperatures than the first thermocouple, contrary to what was expected. This result may be related to the thermocouples placement, because it was difficult to ensure the dimensions of the brazed areas, the thickness of the brazing, as well as the depth in which the thermocouple was brazed. As a consequence of these adversities, the second thermocouple was not properly brazed. It is possible to support this conclusion from the analysis of the second thermocouple graphic, where the noise existence is evident and is only present in the second thermocouple. Contrarily, the reading of the first thermocouple is a good example of the expected temperature rise curve. The graphic of the first thermocouple shows a quick temperature rise during the first thirty seconds of the test, and then the temperature stabilizes and has only a slightly increase during the remaining time of the test. Further, it is important to

note that even existing the vibration phenomenon during the cutting, the reading of the first thermocouple do not show any noise.

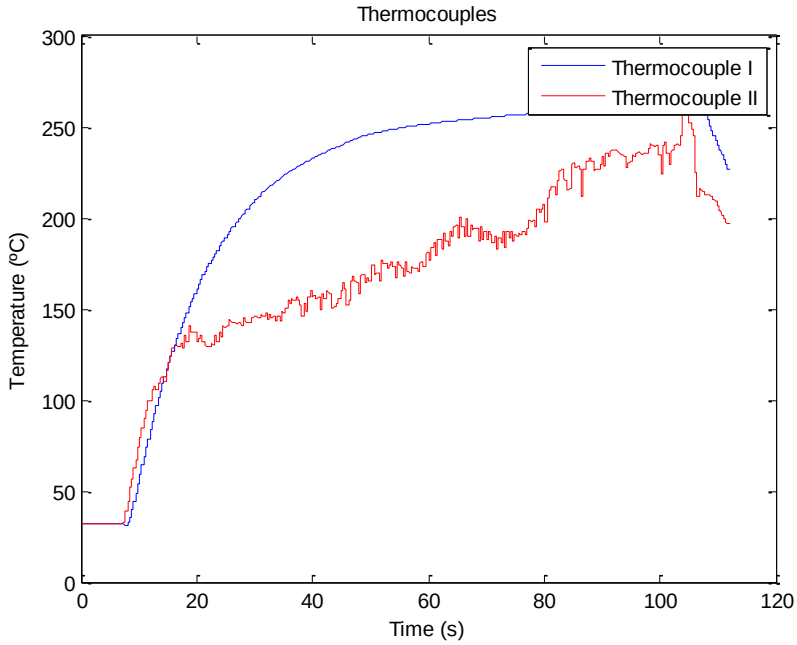

Figure 4.11 - Temperature Measurement: Brazed Thermocouples

5 Conclusions

5.1 Overview and Discussion

In this dissertation was developed an experimental setup to evaluate the forces and the tool temperature distribution in the orthogonal cutting process, by using the materials and equipment available on the mechanical technology laboratory. It was adopted a force measurement technique that used a piezoelectric dynamometer, while the adopted temperature measurement techniques used thermocouples. Furthermore, the performance of the experimental setup was evaluated through tests performed with different materials, different cutting inserts geometries, different cutting parameters, and different attachments of the thermocouples on the cutting insert. The results of the tests performed allowed reaching the following conclusions:

- The adopted force measurement technique did a correct and stable evaluation of the forces during the cutting, although the measurements exhibit some noise caused by the vibration phenomenon;

- The temperature measurement technique with the thermocouples embedded in thermal paste did not perform a correct reading of temperatures. It was concluded that the vibration phenomenon do not allow a correct measurement of temperatures for this technique;

- The temperature measurement technique with the thermocouples embedded in cooper plates presented a better temperature evaluation than the thermocouples embedded in thermal paste, because this second solution provided a better thermal contact. However was verified that the temperature measurements were also strongly affected by the vibration phenomenon;

- The temperature measurement technique in which the thermocouples were brazed in the cutting insert was the solution that gave better temperature evaluations, in which continuous readings of temperature without influence of vibration phenomenon were performed. Although this solution gave a correct reading of temperature, the height and area of the brazing as well as the positioning of the thermocouple inside the brazing affected the temperature measurements. It was concluded that if the thermocouple was improperly brazed the reading was affect by the vibration phenomenon;

- The tests with thermocouples brazed directly in the cutting insert showed that the duration of the tests, even when pre heated, was not sufficient to reach a steady state regime;

- The adopted orthogonal cutting configuration was limited by the disc geometry because this was not able to flow out the heat, and it was concluded that the tests must be shorter.

Concluding, the experimental setup performed accurate measurements of forces, and in what concerns to temperature measurements, accurate measurements were only achieved by the brazed thermocouples. So it was not possible to evaluate the temperature at points, but rather on brazing areas, reason why it would be impossible to determine the temperature distribution along points. Besides, with the adopted orthogonal cutting configuration it was not possible to reach steady state regimes, and therefore it was not possible to determine temperatures rises because the tests ended always before the end of the temperature rise. Therefore the developed experimental setup did not provide a sufficiently robust and reliable performance in order to be adopted in future experimental investigations in metal cutting.

5.2 Suggestions for Future Work

Despite the experimental setup is not yet capable of performing robust and reliable measurements of temperature, it does not mean that this solution should be dropped. Due to the complexity of the thermal contact between the thermocouples and the cutting insert and the time constraints to develop other solutions, further investigations were not possible to implement and test in this dissertation.

In futures works, would be interesting to attach the thermocouples to the cutting insert with micro welding technology, which is available in the Department of Engineering of Materials. Thus, could be possible to study if this attachment solution guarantees a correct positioning of the thermocouples, and consequently a better temperature measurement performance. Another important aspect to improve is to ensure a uniform and effective pre heating of the cutting insert by using different equipment or a different heating method (conduction instead of forced convection).

And after these difficulties are overcome would be interesting to test the experimental setup in order to evaluate its performance with different cutting parameters, different cutting insert geometries and even different work materials. Once a good performance is achieved, the experimental setup may be used to establish a connection between experimental results and theoretical models.

References

[1] P. J. Arrazola, T. Özel, D. Umbrello, M. Davies, and I. S. Jawahir, "Recent advances in modelling of metal machining processes," *CIRP Ann. - Manuf. Technol.*, vol. 62, no. 2, pp. 695–718, 2013.

[2] M. Issa, C. Labergère, K. Saanouni, and a. Rassineux, "Numerical prediction of thermomechanical field localization in orthogonal cutting," *CIRP J. Manuf. Sci. Technol.*, vol. 5, no. 3, pp. 175–195, 2012.

[3] S. Lin, F. Peng, J. Wen, Y. Liu, and R. Yan, "An investigation of workpiece temperature variation in end milling considering flank rubbing effect," *Int. J. Mach. Tools Manuf.*, vol. 73, pp. 71–86, 2013.

[4] R. Komanduri and Z. . Hou, "A review of the experimental techniques for the measurement of heat and temperatures generated in some manufacturing processes and tribology," *Tribol. Int.*, vol. 34, no. 10, pp. 653–682, 2001.

[5] M. a. Davies, T. Ueda, R. M'Saoubi, B. Mullany, and a. L. Cooke, "On The Measurement of Temperature in Material Removal Processes," *CIRP Ann. - Manuf. Technol.*, vol. 56, no. 2, pp. 581–604, 2007.

[6] A. Praça, "Predictive analytical and numerical modeling for orthogonal cutting," Universidade Nova de Lisboa, 2014.

[7] L. P. B. Oxley, *Mechanics of Machinin an analytical approach to assessing machinability*, 1st ed. Chichester, West Sussex: Ellis Hordwood Limited, 1989.

[8] M. E. Merchant, "Mechanics of the metal cutting process. I. Orthogonal cutting and a type 2 chip," *J. Appl. Phys.*, vol. 16, no. 5, pp. 267–275, 1945.

[9] G. Boothroyd and W. A. Knight, *Fundamentals of Machining and Machine Tools*, 2nd ed. New York: Marcel Dekker, INC., 1989.

[10] W. F. Hastings, "A new quick-stop device and grid technique for metal cutting," *Ann. CIRP*, vol. XV, p. 109, 1967.

[11] A. Basti, T. Obikawa, and J. Shinozuka, “Tools with built-in thin film thermocouple sensors for monitoring cutting temperature,” *Int. J. Mach. Tools Manuf.*, vol. 47, no. 5 SPEC. ISS., pp. 793–798, 2007.

[12] D. Werschmoeller and X. Li, “Measurement of tool internal temperatures in the toolchip contact region by embedded micro thin film thermocouples,” *J. Manuf. Process.*, vol. 13, no. 2, pp. 147–152, 2011.

[13] B. Li, L. Li, X. Li, and K. F. Ehmann, “Experimental Investigation of Hard Turning Mechanisms by PCBN Tooling Embedded Micro Thin Film Thermocouples,” *J. Manuf. Sci. Eng.*, vol. 135, no. August 2013, p. 041013, 2013.

[14] M. C. Shaw, *Metal Cutting Principles*, 1st ed. New York: Oxford University Press, 1984.

[15] N. Fang, I. S. Jawahir, and P. L. B. Oxley, “Universal slip-line model with non-unique solutions for machining with curled chip formation and a restricted contact tool,” *Int. J. Mech. Sci.*, vol. 43, no. 2, pp. 557–580, 2001.

[16] A. P. Markopoulos, “Finite Element Method in Machining Processes,” pp. 71–92, 2013.

[17] R. Komanduri and Z. B. Hou, “Thermal modeling of the metal cutting process - Part I : temperature rise distribution due to shear plane heat source,” vol. 42, no. 2000, pp. 1715–1752, 1999.

[18] N. a. Abukhshim, P. T. Mativenga, and M. a. Sheikh, “Heat generation and temperature prediction in metal cutting: A review and implications for high speed machining,” *Int. J. Mach. Tools Manuf.*, vol. 46, no. 7–8, pp. 782–800, 2006.

[19] R. Komanduri and Z. B. Hou, “Thermal modeling of the metal cutting process - Part II : temperature rise distribution due to frictional heat source at the tool - chip interface,” vol. 43, pp. 57–88, 2002.

[20] D. O’Sullivan and M. Cotterell, “Temperature measurement in single point turning,” *J. Mater. Process. Technol.*, vol. 118, no. 1–3, pp. 301–308, 2001.

[21] D. A. Stephenson and J. S. Agapiou, *Mettal Cutting Theory and Practice*, 1st ed. New York: Marcel Dekker, INC., 1997.

[22] Y. Dogu, E. Aslan, and N. Camuscu, “A numerical model to determine temperature distribution in orthogonal metal cutting,” *J. Mater. Process. Technol.*, vol. 171, no. 1, pp. 1–9, 2006.

[23] J. W. Dally, W. F. Riley, and K. G. McConnell, *Instrumentation for Engennering Measurements*, 1st ed. Singapure: John Wiley & Sons, INC., 1984.

[24] J. J. P. Teixeira, *Fundamentos Físicos do Corte dos Metais*. Universidade Nova de Lisboa, 2001.

[25] “RS, Amidata S.A.,” 2014. [Online]. Available: http://docs-europe.electrocomponents.com/webdocs/0800/0900766b80800a84.pdf. [Accessed: 02-Jul-2014].

Appendix

This appendix presents the technical drawings of the produced components and specimens.

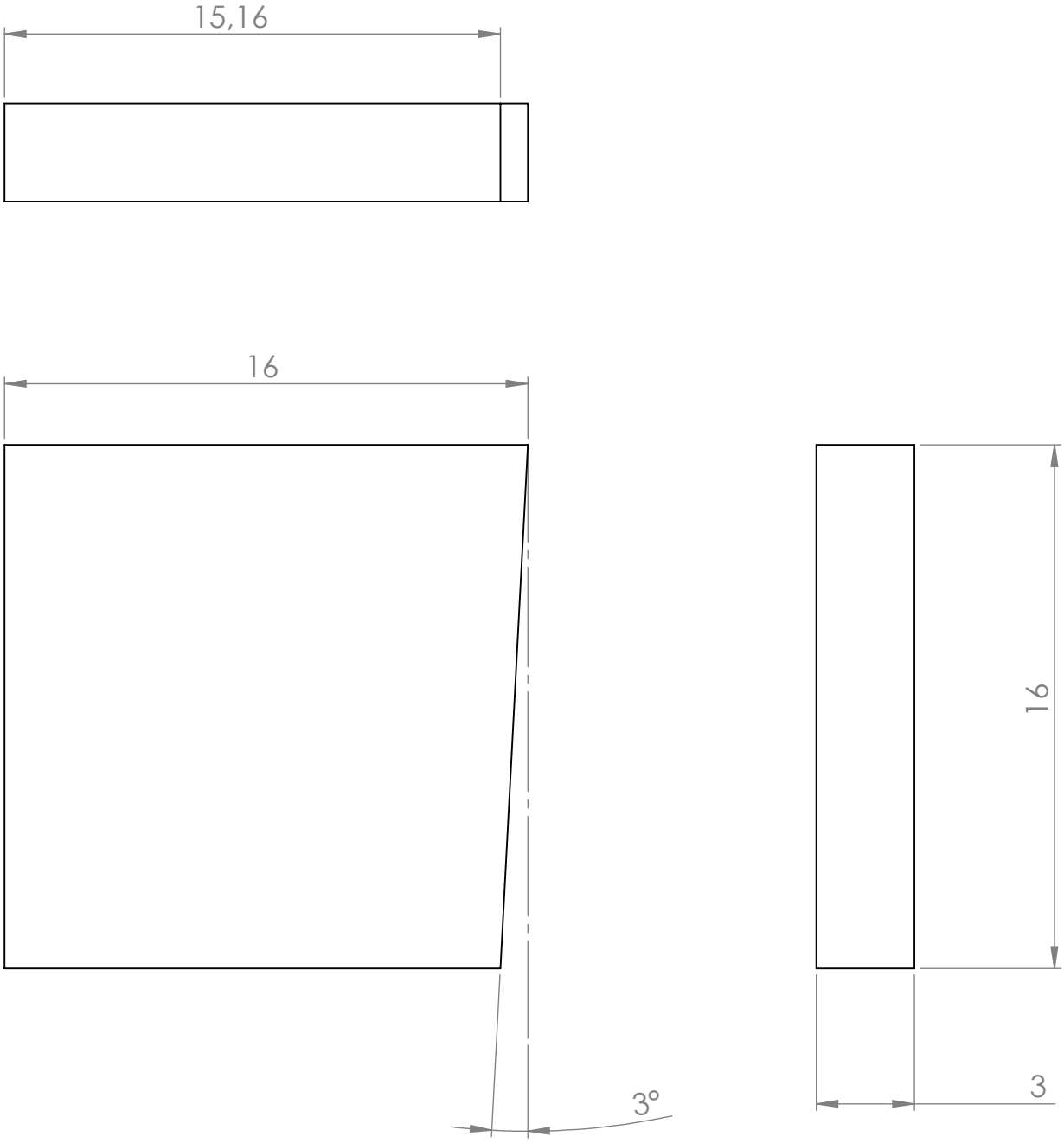

UNLESS OTHERWISE SPECIFIED: DIMENSIONS ARE IN MILLIMETERS SURFACE FINISH: TOLERANCES: LINEAR: ANGULAR:	FINISH:		DEBUR AND BREAK SHARP EDGES		DO NOT SCALE DRAWING	REVISION
	NAME	SIGNATURE	DATE		TITLE:	
DRAWN					Cutting Insert Type I	
CHK'D						
APPV'D						
MFG						
Q.A				MATERIAL:	DWG NO.	A4
				WEIGHT:	SCALE:5:1	SHEET 1 OF 1

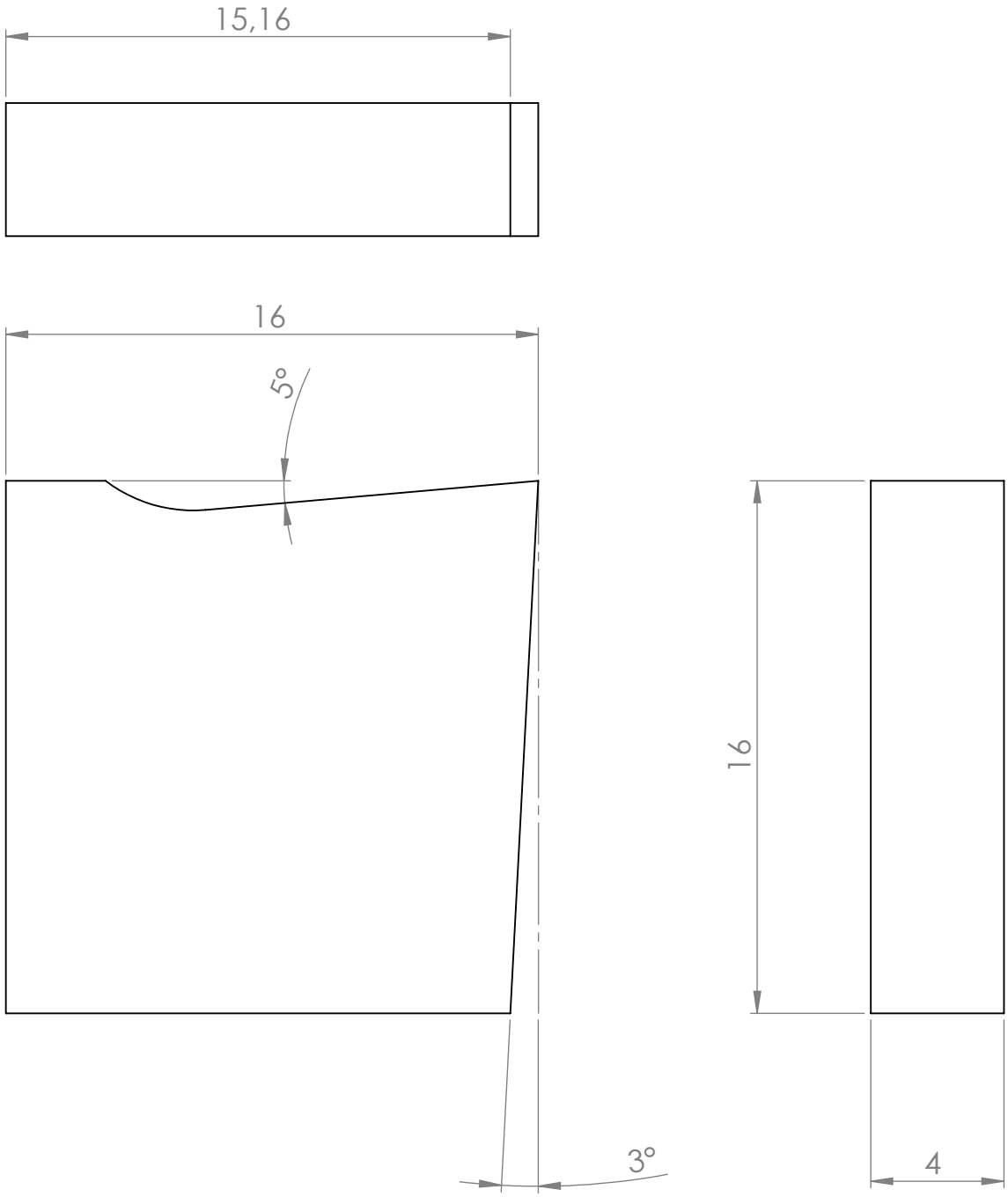

UNLESS OTHERWISE SPECIFIED: DIMENSIONS ARE IN MILLIMETERS SURFACE FINISH: TOLERANCES: LINEAR: ANGULAR:	FINISH:		DEBUR AND BREAK SHARP EDGES	DO NOT SCALE DRAWING	REVISION	
	NAME	SIGNATURE	DATE	TITLE:		
DRAWN				Cutting Insert Type II		
CHK'D						
APPV'D						
MFG						
Q.A				MATERIAL:	DWG NO.	A4
				WEIGHT:	SCALE:5:1	SHEET 1 OF 1

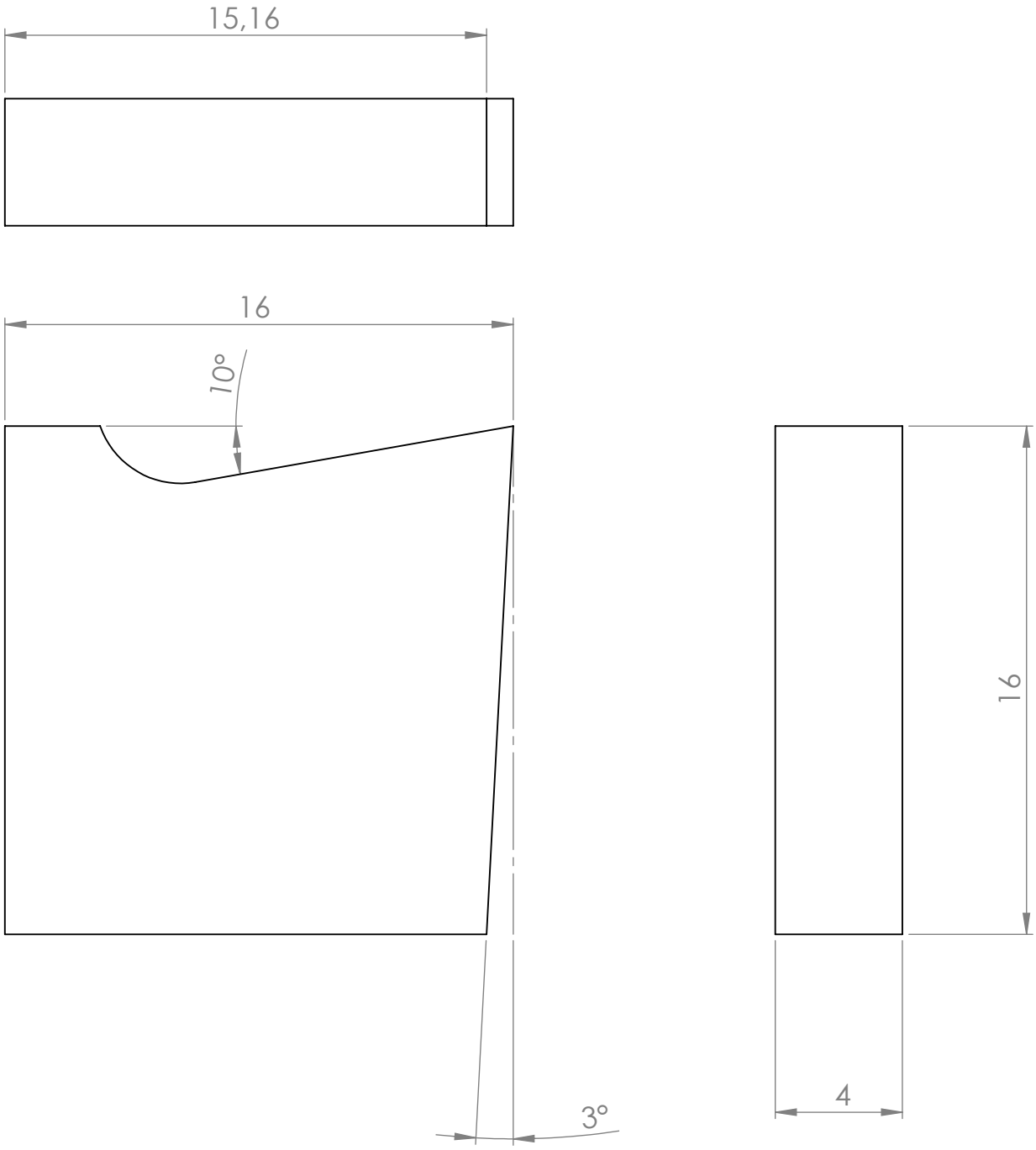

UNLESS OTHERWISE SPECIFIED: DIMENSIONS ARE IN MILLIMETERS SURFACE FINISH: TOLERANCES: LINEAR: ANGULAR:	FINISH:		DEBUR AND BREAK SHARP EDGES		DO NOT SCALE DRAWING	REVISION
	NAME	SIGNATURE	DATE		TITLE:	
DRAWN					Cutting Insert Type III	
CHK'D						
APPV'D						
MFG						
Q.A				MATERIAL:	DWG NO.	A4
				WEIGHT:	SCALE:5:1	SHEET 1 OF 1

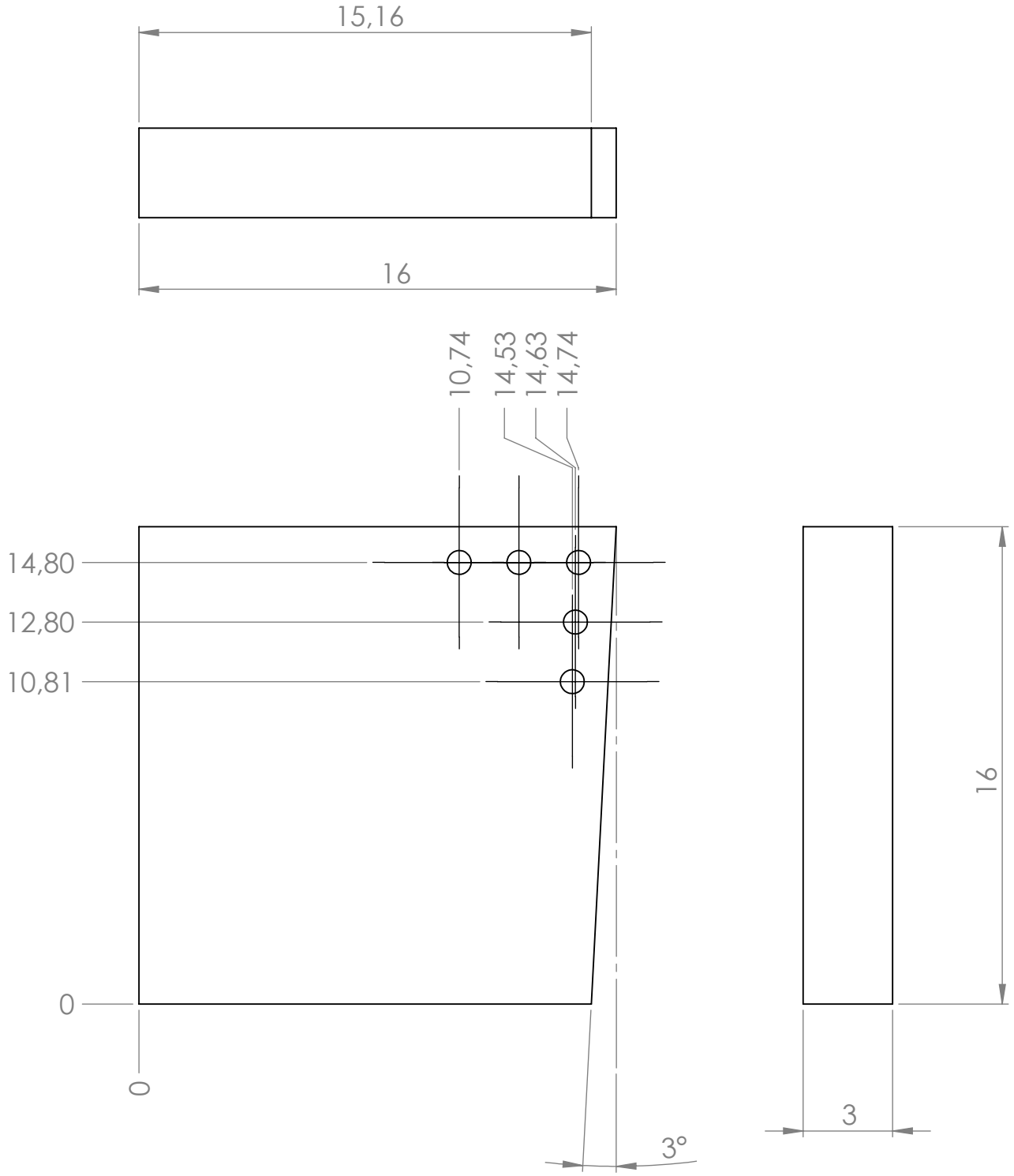

UNLESS OTHERWISE SPECIFIED: DIMENSIONS ARE IN MILLIMETERS SURFACE FINISH: TOLERANCES: LINEAR: ANGULAR:	FINISH:		DEBUR AND BREAK SHARP EDGES		DO NOT SCALE DRAWING	REVISION
	NAME	SIGNATURE	DATE		TITLE:	
DRAWN					Thermocouples Positioning Insulating Type I	
CHK'D						
APPV'D						
MFG						
Q.A				MATERIAL:	DWG NO.	A4
				WEIGHT:	SCALE:5:1	SHEET 1 OF 1

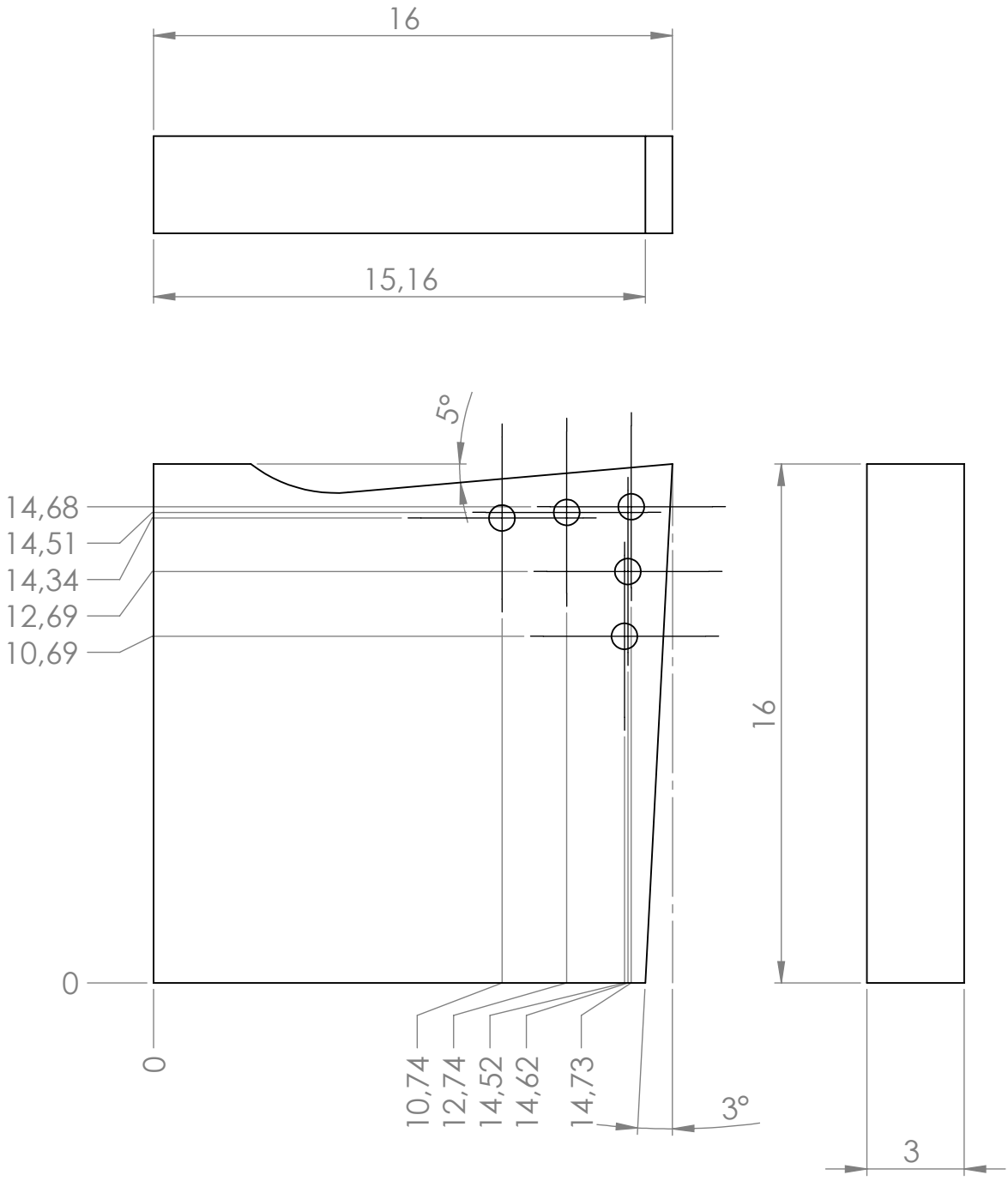

UNLESS OTHERWISE SPECIFIED: DIMENSIONS ARE IN MILLIMETERS SURFACE FINISH: TOLERANCES: LINEAR: ANGULAR:	FINISH:		DEBUR AND BREAK SHARP EDGES	DO NOT SCALE DRAWING	REVISION	
	NAME	SIGNATURE	DATE	TITLE:		
DRAWN				Thermocouples Positioning Insulating Type II		
CHK'D						
APPV'D						
MFG						
Q.A				MATERIAL:	DWG NO.	A4
				WEIGHT:	SCALE:5:1	SHEET 1 OF 1

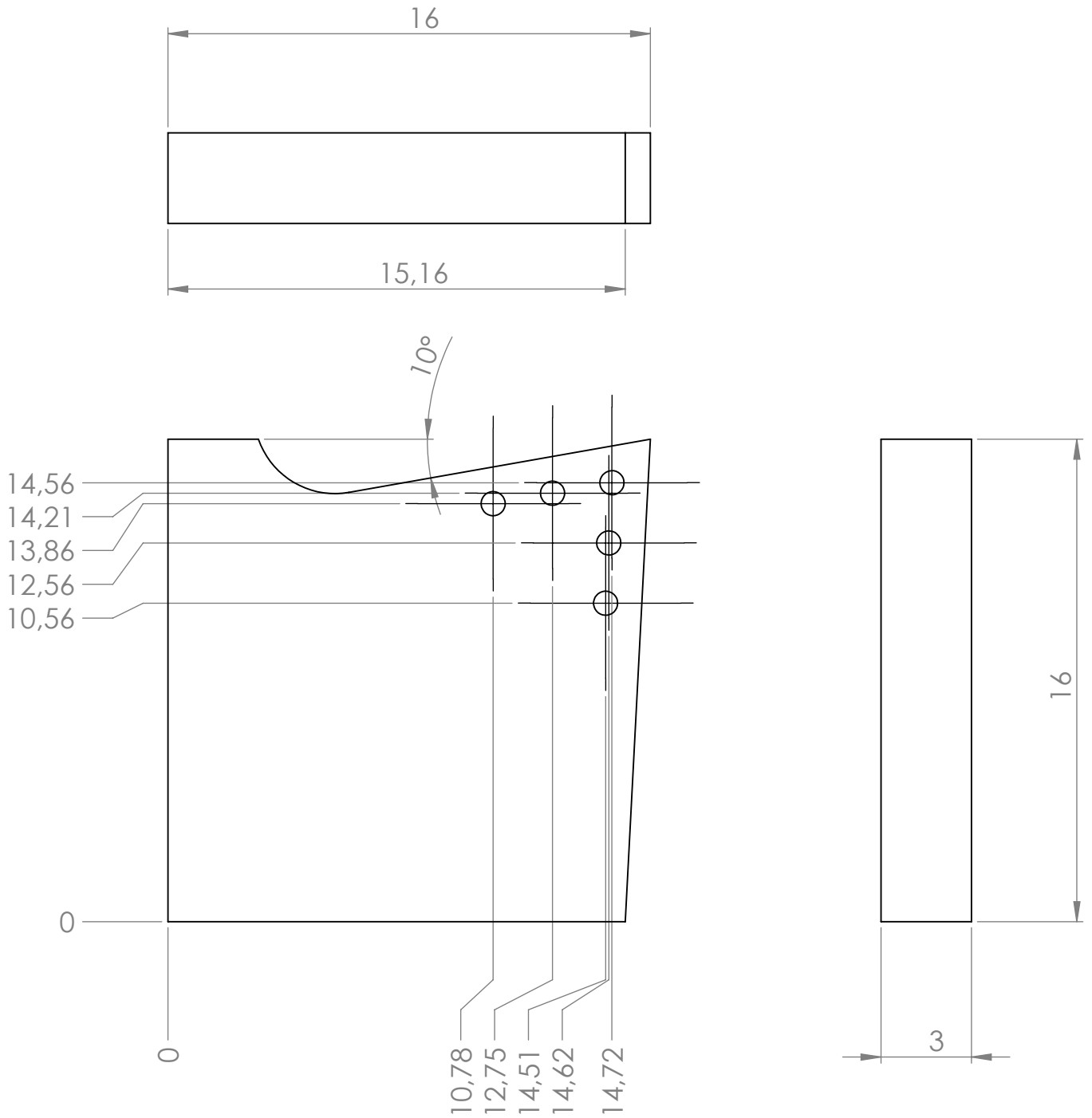

UNLESS OTHERWISE SPECIFIED: DIMENSIONS ARE IN MILLIMETERS SURFACE FINISH: TOLERANCES: LINEAR: ANGULAR:	FINISH:		DEBUR AND BREAK SHARP EDGES		DO NOT SCALE DRAWING	REVISION
	NAME	SIGNATURE	DATE		TITLE: Thermocouples Positioning Insulating Type III	
DRAWN						
CHK'D						
APPV'D						
MFG						
Q.A				MATERIAL:	DWG NO.	A4
				WEIGHT:	SCALE:5:1	SHEET 1 OF 1

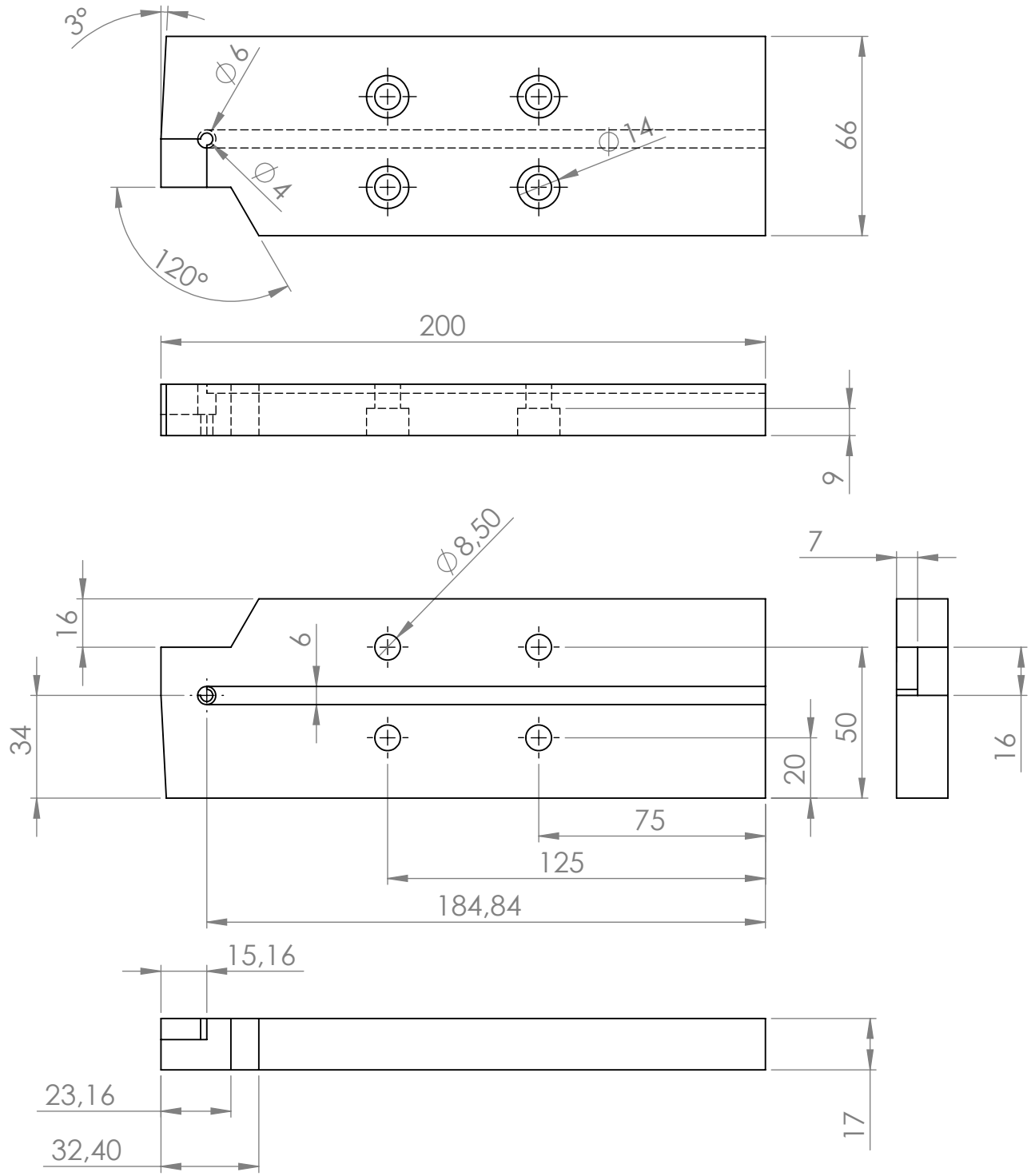

UNLESS OTHERWISE SPECIFIED: DIMENSIONS ARE IN MILLIMETERS SURFACE FINISH: TOLERANCES: LINEAR: ANGULAR:	FINISH:		DEBUR AND BREAK SHARP EDGES		DO NOT SCALE DRAWING	REVISION
	NAME	SIGNATURE	DATE			TITLE:
DRAWN						Tool Holder
CHK'D						
APPV'D						
MFG						
Q.A				MATERIAL:		DWG NO. A4
				WEIGHT:		SCALE:1:2 SHEET 1 OF 1

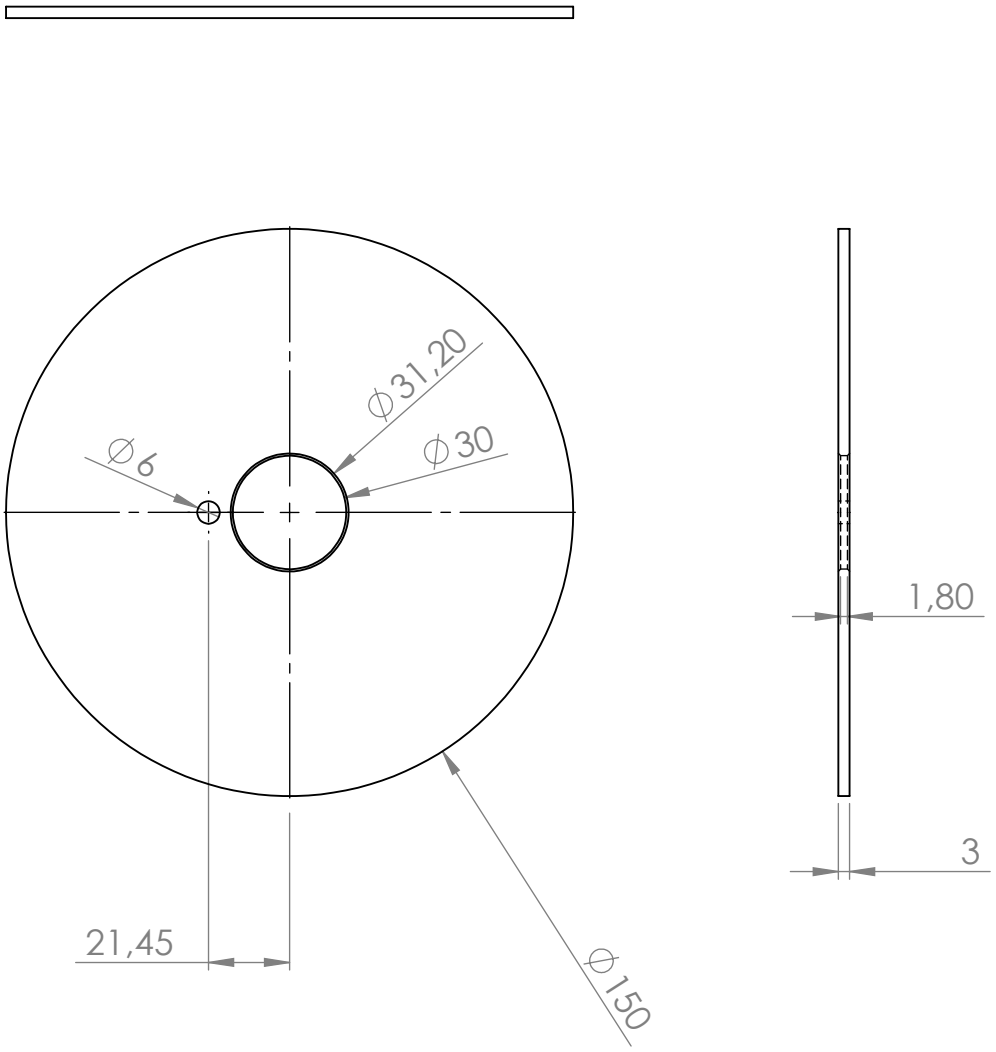

UNLESS OTHERWISE SPECIFIED: DIMENSIONS ARE IN MILLIMETERS SURFACE FINISH: TOLERANCES: LINEAR: ANGULAR:	FINISH:		DEBUR AND BREAK SHARP EDGES		DO NOT SCALE DRAWING	REVISION
	NAME	SIGNATURE	DATE		TITLE:	
DRAWN					Thin Disc	
CHK'D						
APPV'D						
MFG						
Q.A				MATERIAL: AISI 304L / 42 Cr Mo 4 / AISI 1020	DWG NO.	A4
				WEIGHT:	SCALE:1:2	SHEET 1 OF 1

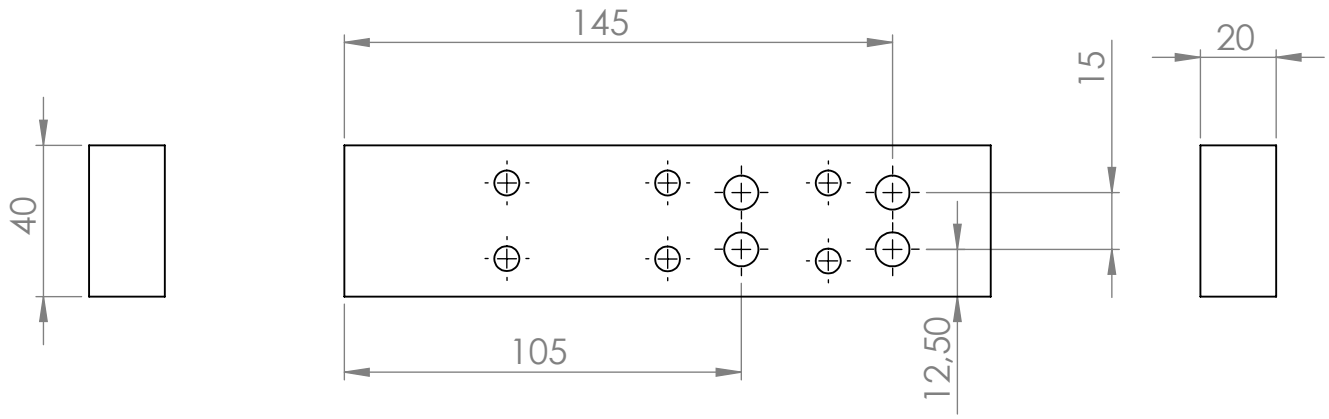

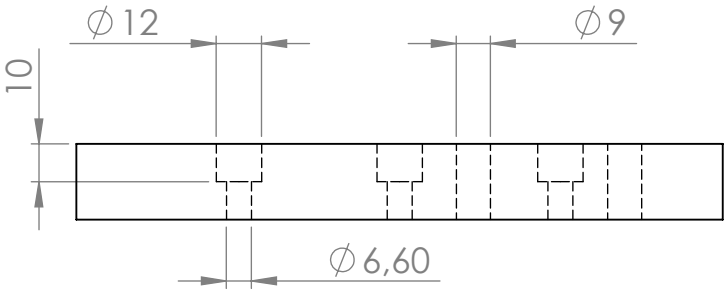

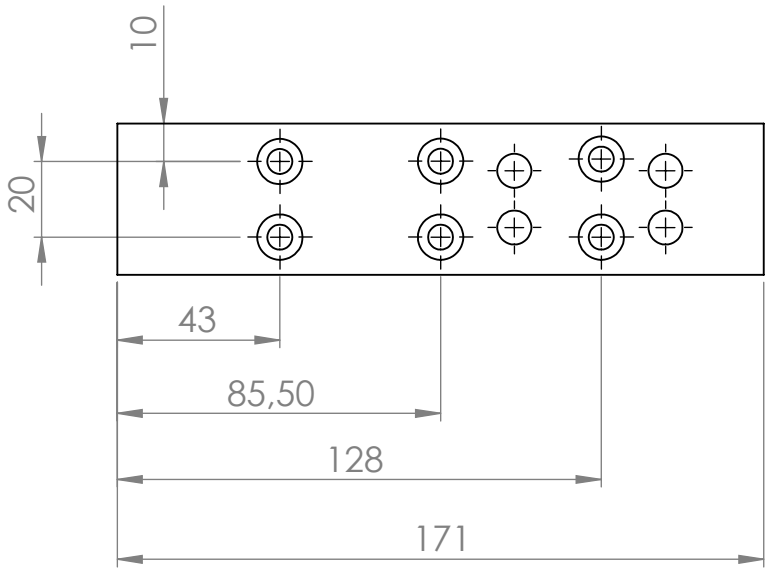

UNLESS OTHERWISE SPECIFIED: DIMENSIONS ARE IN MILLIMETERS SURFACE FINISH: TOLERANCES: LINEAR: ANGULAR:	FINISH:		DEBUR AND BREAK SHARP EDGES		DO NOT SCALE DRAWING	REVISION
	NAME	SIGNATURE	DATE		TITLE:	
DRAWN					Dynamometer Fixing System - Component I	
CHK'D						
APPV'D						
MFG						
Q.A				MATERIAL:	DWG NO.	A4
				WEIGHT:	SCALE:1:2	SHEET 1 OF 1

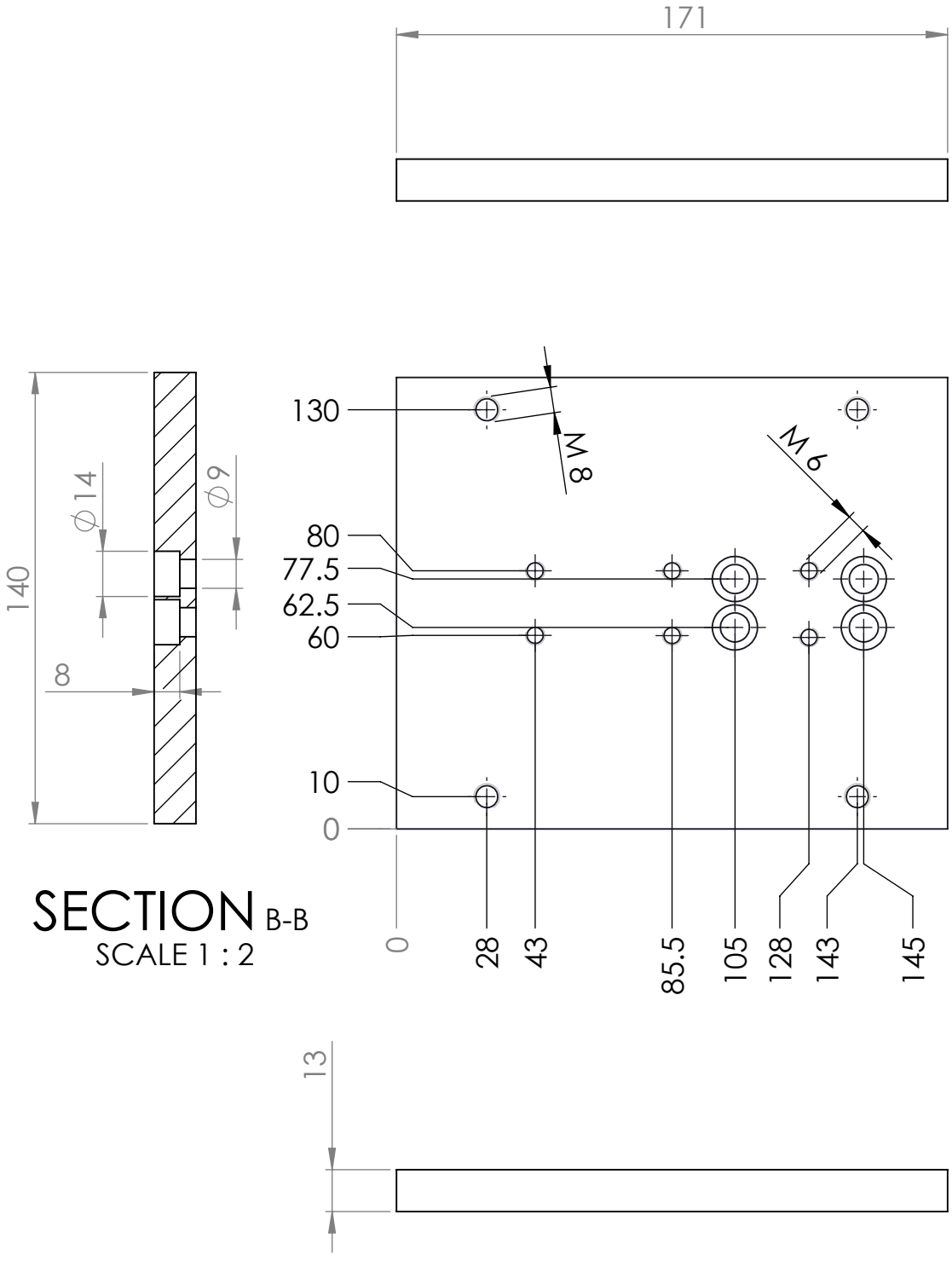

UNLESS OTHERWISE SPECIFIED: DIMENSIONS ARE IN MILLIMETERS SURFACE FINISH: TOLERANCES: LINEAR: ANGULAR:	FINISH:		DEBUR AND BREAK SHARP EDGES	DO NOT SCALE DRAWING	REVISION	
	NAME	SIGNATURE	DATE	TITLE:		
DRAWN				Dynamometer Fixing System - Component II		
CHK'D						
APPV'D						
MFG						
Q.A				MATERIAL:	DWG NO.	A4
				WEIGHT:	SCALE:1:5	SHEET 1 OF 1

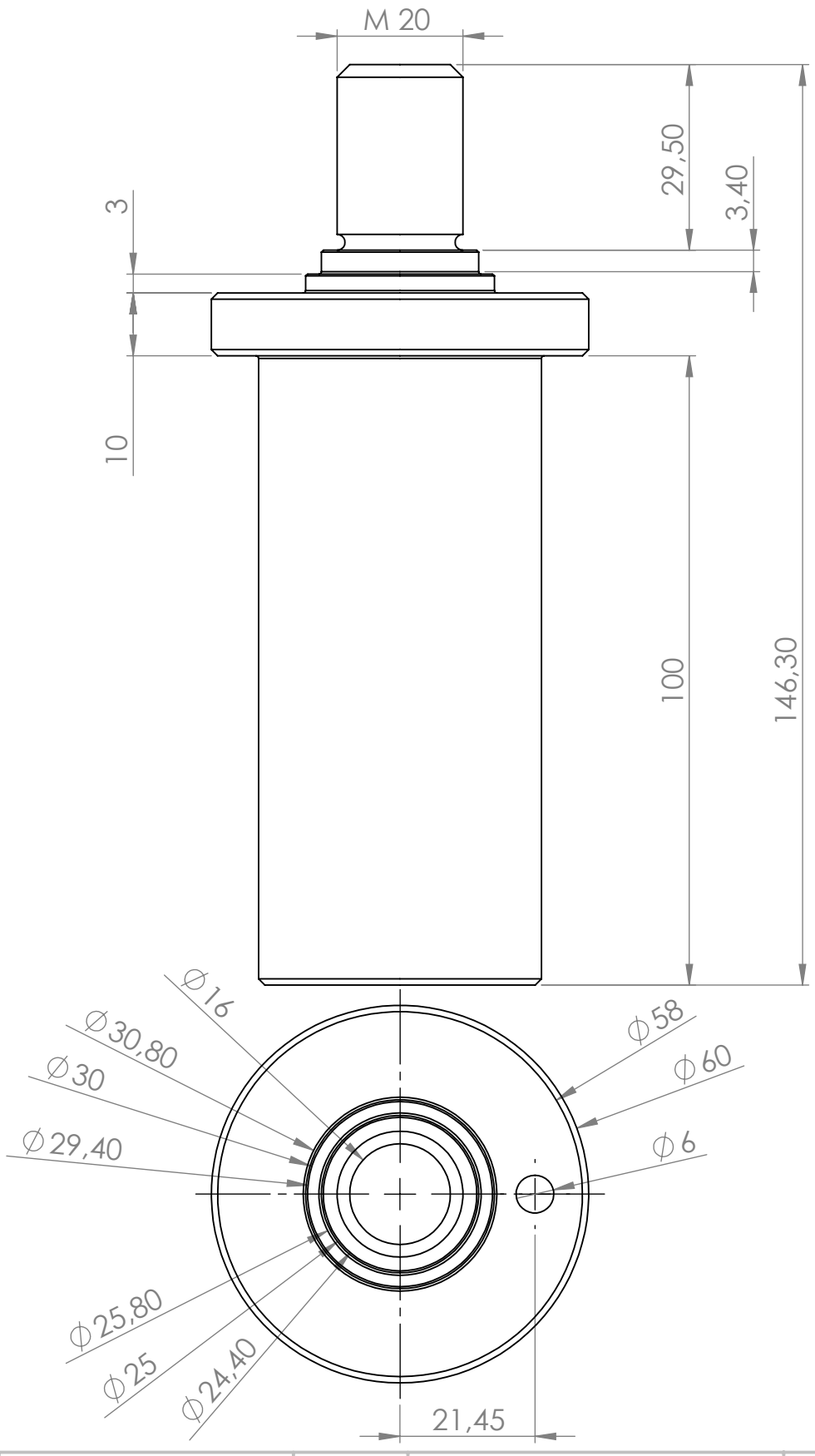

UNLESS OTHERWISE SPECIFIED: DIMENSIONS ARE IN MILLIMETERS SURFACE FINISH: TOLERANCES: LINEAR: ANGULAR:	FINISH:		DEBUR AND BREAK SHARP EDGES		DO NOT SCALE DRAWING	REVISION
	NAME	SIGNATURE	DATE			TITLE:
DRAWN						Mandrel
CHK'D						
APPV'D						
MFG						
Q.A				MATERIAL:		DWG NO. A4
				WEIGHT:		SCALE:1:2 SHEET 1 OF 1

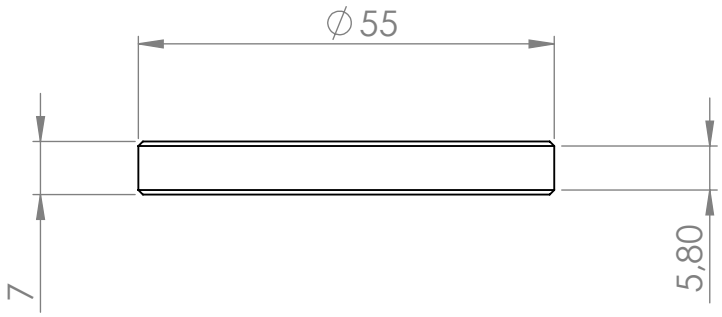

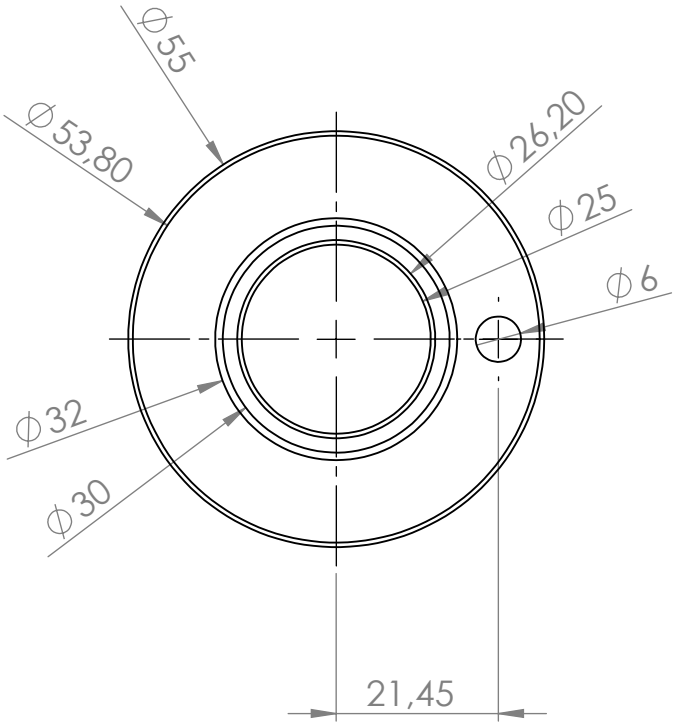

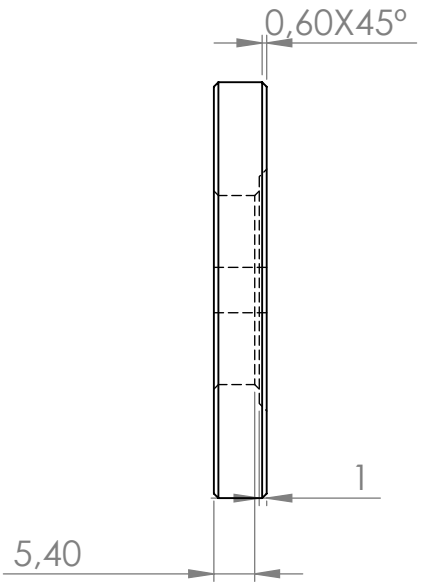

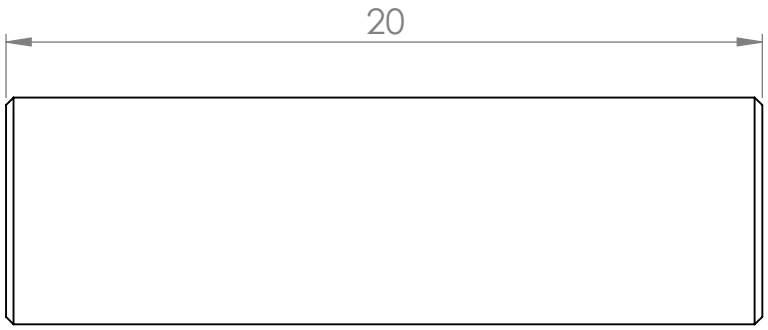

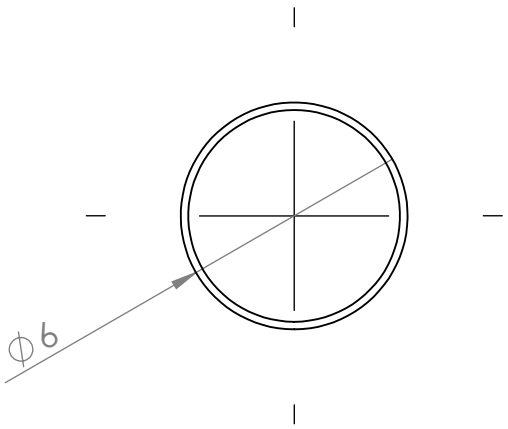

UNLESS OTHERWISE SPECIFIED: DIMENSIONS ARE IN MILLIMETERS SURFACE FINISH: TOLERANCES: LINEAR: ANGULAR:	FINISH:		DEBUR AND BREAK SHARP EDGES	DO NOT SCALE DRAWING	REVISION	
	NAME	SIGNATURE	DATE	TITLE:		
DRAWN				Washer and Pin		
CHK'D						
APPV'D						
MFG						
Q.A				MATERIAL:	DWG NO.	A4
				WEIGHT:	SCALE:1:1	SHEET 1 OF 1